

Novel Agonists and Antagonists for Human Protease Activated Receptor 2

Grant D. Barry,[†] Jacky Y. Suen,[†] Giang T. Le, Adam Cotterell, Robert C. Reid, and David P. Fairlie*

Division of Chemistry and Structural Biology, Institute for Molecular Bioscience, The University of Queensland, Brisbane Qld 4072, Australia. [†]Joint first authors.

Received July 31, 2010

Human protease activated receptor 2 (PAR2) is a G protein-coupled receptor that is associated with inflammatory diseases and cancers. PAR2 is activated by serine proteases that cleave its N-terminus and by synthetic peptides corresponding to the new N-terminus. Peptide agonists are widely used to characterize physiological roles for PAR2 but typically have low potency (e.g., SLIGKV-NH₂, SLIGRL-NH₂), uncertain target selectivity, and poor bioavailability, limiting their usefulness for specifically interrogating PAR2 in vivo. Structure–activity relationships were used to derive new PAR2 agonists and antagonists containing nonpeptidic moieties. Agonist GB110 (**19**, EC₅₀ 0.28 μM) selectively induced PAR2-, but not PAR1-, mediated intracellular Ca²⁺ release in HT29 human colorectal carcinoma cells. Antagonist GB83 (**36**, IC₅₀ 2 μM) is the first compound at micromolar concentrations to reversibly inhibit PAR2 activation by both proteases and other PAR2 agonists (e.g., trypsin, 2f-furoyl-LIGRLO-NH₂, **19**). The new compounds are selective for PAR2 over PAR1, serum stable, and suitable for modulating PAR2 in disease models.

Introduction

Among the most unusual of almost 1000 known human G protein-coupled receptors (GPCRs^a)^{1,2} are four protease activated receptors (PARs),^{3,4} which have no known endogenous extracellular ligands. Instead, serine proteases indirectly activate at least four PAR subtypes by cleaving their N-terminus, exposing a new extracellular N-terminus that folds back onto and intramolecularly self-activates PAR.⁵ Research on PARs has focused on PAR1 because it is a receptor for the serine protease thrombin, and thus a potential therapeutic target in cardiovascular disease.³ PAR2 is not activated by thrombin, but it is activated by other serine proteases (e.g., trypsin, tryptase,

cathepsin G) and has been linked to inflammatory and proliferative disorders.^{3–7}

Most PAR2 research has attempted to define physiological and pathophysiological roles for this receptor. Distributed widely throughout the body, PAR2 signals through intracellular G proteins^{3,8} associated with release of intracellular Ca²⁺ via phospholipase C activation and inositol triphosphate (Gα_q),⁸ p38 MAP kinase and ERK phosphorylation, as well as adenylyl cyclase inhibition (Gα_i),^{9–11} and Rho-dependent phagocytosis (Gα_{12/13}).¹² PAR2 activation has been linked to proliferation, metastasis, and angiogenesis in many cancers especially of the stomach,¹³ colon,^{11,14} breast, and pancreas.^{11,15–17} PAR2 has been implicated as a pro-inflammatory mediator in arthritis,¹⁸ inflammatory bowel disease,^{19,20} pancreatitis,^{21–27} and cardiovascular disease,²⁸ while it has also been reported as anti-inflammatory and protective in other conditions such as gastric ulcer,²⁹ colitis,³⁰ asthma,^{27,31–33} and liver fibrosis.^{30,34–36} Clearly, these roles are not yet well understood.^{22,24–26,37}

PAR2^{-/-} deficient mice show delayed appearance and decreased development of mammary adenocarcinoma³⁸ and abolished revascularization in hypoxia-induced angiogenesis.³⁹ In inflammation, PAR2 knockouts had reduced dendritic cell trafficking and T cell activation,⁴⁰ and higher survival against antiphospholipid syndrome by lowered neutrophil activation.⁴¹ PAR2 deficient mice also had impaired production of IgE and IL-4,⁴² reduced contact sensitivity in airway inflammation,⁴³ resistance to adjuvant-induced arthritis,¹⁸ or delayed onset of inflammation.⁴⁴ Roles for PAR2 in inflammation were further supported by studies with small interfering RNA (siRNA) for PAR2, which repeatedly showed suppression of innate immunity markers, such as IL8,^{40,45} CXCL5, and CCL20.⁴⁶ By contrast, PAR2 activation attenuated pancreatitis-related hyperalgesia,⁴⁷ and thus, the role of PAR2 could be cell type-specific. This is supported by a

*To whom correspondence should be addressed. Telephone: +61-733462989. Fax: +61 733462990. E-mail: d.fairlie@imb.uq.edu.au.

^a Abbreviations: ACN, acetonitrile; Boc, *tert*-butoxycarbonyl; BOP, (benzotriazol-1-yloxy)-tris(dimethylamino) phosphonium hexafluorophosphate; Cha, cyclohexylalanine; DCM, dichloromethane; DIC, 1,3-diisopropylcarbodiimide; DIPEA, *N,N*-diisopropylethylamine; DMF, *N,N*-dimethylformamide; DMSO, dimethyl sulfoxide; DTPM, 1,3-dimethyl-5-[(dimethylamino)methylene]-2,4,6-(1H,3H,5H)-trioxopyrimidine; EC₅₀, molar concentration that produces 50% of the maximum response of an agonist; ERK, extracellular signal-regulated kinase; ESMS, electrospray mass spectroscopy; FCS, fetal calf serum; Fmoc, 9H-fluoren-9-ylmethoxycarbonyl; GI, gastrointestinal, G protein, guanosine monophosphate-protein; GPCR, G protein-coupled receptor; HBSS, Hank's balanced salt solution; HEK293, human embryonic kidney 293 cells; HBTU, *O*-(1H-benzotriazol-1-yl)-1,1,3,3-tetramethyluronium hexafluorophosphate; HEPES, 4-(2-hydroxyethyl)-1-piperazineethanesulfonic acid; HOBt, 1-hydroxybenzotriazole; HT29, human colon adenocarcinoma grade II cells; HRMS, high resolution mass spectroscopy; IC₅₀, molar concentration of an antagonist that inhibits 50% of a known concentration of agonist activity; IgE, immunoglobulin E; IL, interleukin; IMDM, Iscove's modified Dulbecco's medium; iCa²⁺, intracellular Ca²⁺; MAP kinase, mitogen-activated protein kinase; MBHA, methylbenzhydrylamine; PAR, protease activated receptor; rpHPLC, reversed phase high performance liquid chromatography; SAR, structure–activity relationships; siRNA, small interfering ribonucleic acid; SEM, standard error of mean; SPPS, solid phase peptide synthesis; TFA, trifluoroacetic acid; TIPS, triisopropylsilane; TCP, tritylchloride-polystyrene.

protective role for PAR2 on neurons, yet a pathogenic role on glial cells in Alzheimer's disease.⁴⁸ PAR2 antibodies are available to sequences upstream of the PAR2 cleavage site, across the cleavage site, at the newly exposed N-terminus, and at the C-terminus, but they have not been extensively used in PAR2 research due to their lack of selectivity. Some studies have shown that PAR2 interaction with tissue factors is important for tumor growth.⁴⁹

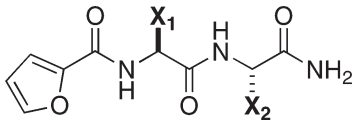
Trypsin is a potent activator of PAR2 in the GI tract where pancreatic trypsin is found, and in colon, airway epithelium, neuronal, and vascular endothelial cells and skin, intestine, kidney, and pancreas where trypsinogen expression has been demonstrated.⁵⁰ However, like other serine proteases, trypsin nonspecifically cleaves many proteins in addition to PAR2. Thus, much of the evidence for PAR2 in disease has had to rely upon the use of short synthetic hexapeptides, corresponding to the new N-terminal sequence of PAR2 exposed after proteolytic cleavage. Hexapeptides SLIGKV-NH₂ and SLIGRL-NH₂, corresponding to the tethered ligand human and murine sequences, respectively, can activate human PAR2 at micromolar concentrations without the need for proteases which are much more potent agonists (nM).³ Due to their low potency, these short peptide agonists have been administered at high concentrations to elicit responses⁵¹ and, although selective for PAR2 over PAR1, at such high concentrations these peptides also interact with other receptors.^{52,53} Similarly, the first known antagonist of protease-activated PAR2 has only millimolar affinity for PAR2 and selectivity is most unlikely.⁵⁴ A second antagonist reported for PAR2 is active at micromolar concentrations but is completely inactive against endogenous activators like the serine protease trypsin.⁵⁵ Our understanding of PAR2 physiology is thus still quite limited by the lack of truly selective and potent PAR2 agonists and antagonists suitable for in vivo studies.

More potent peptide agonists have been created for PAR2.^{56–64} Hexapeptide analogues in which serine is replaced by 2-furoyl (e.g., 2-furoyl-LIGRL-NH₂),^{61,62} a residue is added to the seventh position (e.g., SLIGRLI-NH₂),^{63,64} the sixth residue is changed to *para*-nitrophenylalanine (e.g., SLIGR(pNO₂F)I-NH₂),⁶⁴ or combinations of these N- and C-terminal changes have 5–30-fold higher agonist potency than SLIGRL-NH₂ and are selective for PAR2 over PAR1. Other heterocyclic replacements for serine can also result in equipotent PAR2 agonists,⁶⁴ while large aromatic groups in place of the C-terminal leucine impart a similar enhancement in PAR2 agonist potency. Screening of 250,000 druglike compounds produced two small molecule agonists of PAR2 with similar potency to 2-furoyl-LIGRL-NH₂, some selectivity for PAR₂, and metabolic stability in vivo.^{65,66} Although down-sizing agonist peptides derived from SLIGRL-NH₂ has been found to reduce PAR2 agonist potency,⁵⁸ this was not the case for more potent agonist peptides with heterocyclic replacements for serine at the N-terminus. The present study began with a heterocyclic replacement for the N-terminal serine, then truncation and optimization of very short peptides with selective PAR2 agonist potency, before altering the C-terminus with nonpeptidic fragments that dictate agonist or antagonist potency.

Results and Discussion

Truncating PAR2 Activating Peptides. A series of short peptide agonists 1–7 (Table 1), featuring a heterocyclic replacement for serine at the N-terminus, was synthesized by standard solid phase methodology on Rink amide MBHA

Table 1. Intracellular Ca²⁺ Release by 1–7 in HT29 Cells



compd (50 μM)	X ₁	X ₂	% relative activity ^a
1	Leu	Ile	38 ± 5
2	Leu	Cha	43 ± 1
3	Leu	Phe	22 ± 2
4	Leu	Phe(<i>p</i> -F)	19 ± 3
5	Cha	Ile	58 ± 10
6	Phe	Ile	67 ± 2
7	Chg	Ile	12 ± 1

^a Versus 100% iCa²⁺ release induced by 2f-LIGRLI-NH₂ (50 μM).⁶⁴

resin using Fmoc-protected amino acids. The intention was to identify the minimum number of residues required for PAR2 activity. Compounds were evaluated at a single concentration (50 μM) for induction of intracellular Ca²⁺ (iCa²⁺) release in HT29 colon cancer cells relative to the calcium efflux produced by a PAR2 agonist, 2-furoyl-LIGRLI-NH₂ (2f-LIGRLI-NH₂),⁶⁴ at the same concentration (Table 1). Compounds were not active enough to determine EC₅₀, being too insoluble above 50 μM to test at higher concentrations. Table 1 shows that bulky amino acids linked to the 2-furoyl group have some agonist activity, with cyclic aliphatic or aromatic side chains being preferred at position X₁ (**5**, **6** vs **1**), while shortening the aliphatic side chain (**7**) was detrimental.

Compounds **5** and **6** were next evaluated for PAR2 versus PAR1 selectivity in order to choose between them for further synthetic elaboration. In hexapeptide agonists based on SLIGRL, substitution of leucine 2 with phenylalanine but not cyclohexylalanine has been reported to favor binding to PAR1 on HEK293 cells, thereby reducing PAR2 selectivity.^{3,59} A receptor desensitization assay⁶⁷ was therefore performed (Figure 1) by treating HEK293 cells with PAR2 agonist⁶⁴ 2f-LIGRLI-NH₂ (6.7 μM) followed by a second treatment with the same agonist after 6 min (*t*₃₇₀) to re-establish a baseline (7.5 μM final concentration, Figure 1A), consistent with desensitization of PAR2. Alternatively, if the second treatment at *t*₃₇₀ was with the PAR1-selective weak agonist TFLLR-NH₂ (80 μM), calcium efflux was observed since PAR1 had not been desensitized by prior treatment with PAR2 agonist (Figure 1B). In a parallel experiment, cells were treated with 80 μM **5** or **6** at *t*₃₇₀ following desensitization of the PAR2 receptors with 2f-LIGRLI-NH₂. Lack of a second calcium efflux following treatment with **5** (Figure 1C) indicated PAR2 selective activation, whereas **6** induced a calcium response (Figure 1D), suggesting no PAR2 selectivity and activation of another receptor(s). The same experiment in which cells were first desensitized by treatment with 100 μM PAR1 selective agonist TFLLR-NH₂ (Figure 1E, F) showed that **6** was activating mainly through PAR1, whereas **5** was capable of inducing a PAR1-independent Ca²⁺ response consistent with selectivity for PAR2 over PAR1.

Our previous SAR studies⁶⁴ with PAR2 activating hexapeptides on HEK293 cells indicated that serine could be replaced by several heterocyclic alternatives to the 2-furoyl group. We therefore compared Ca²⁺ efflux in HEK293 cells in response to **5** (EC₅₀ > 50 μM, *n* = 3) and analogues in which the furoyl group was replaced with pyrazoyl (**8**, EC₅₀ > 100 μM,

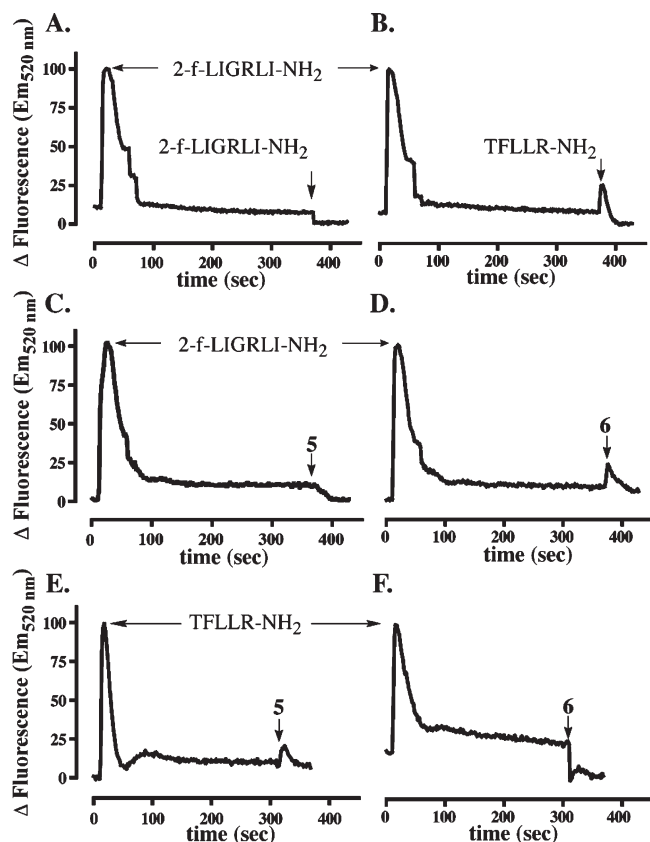
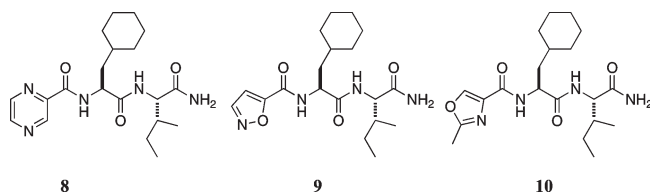


Figure 1. PAR2 versus PAR1 selectivity via receptor desensitization. (A) Treatment of HEK293 cells (t_{10}) with PAR2 selective agonist 2f-LIGRLI-NH₂ (6.7 μ M), followed by second treatment at t_{370} (7.5 μ M final conc) showing desensitization. (B) After initial treatment at t_{10} with 2f-LIGRLI-NH₂, cells were treated with PAR1 selective agonist TFLLR-NH₂ (80 μ M) at t_{370} , showing Ca²⁺ release. Cells desensitized with 2f-LIGRLI-NH₂ (6.7 μ M, t_{10}) were then treated at t_{370} with 80 μ M PAR2 ligand 5 (C) or nonselective 6 (D). Cells desensitized at t_{10} with the PAR1 selective TFLLR-NH₂ (100 μ M) were then treated at t_{310} with 80 μ M 5 (E), suggesting no PAR1 activation, or 6 (F) that activates PAR1.

$n = 3$), isoxazolyl (**9**, EC₅₀ 4 μ M, $n = 3$), or methyloxazolyl (**10**, EC₅₀ > 100 μ M, $n = 3$). The most active compound **9** was the only compound soluble enough at ≤ 100 μ M concentrations to permit determination of a reliable EC₅₀ by varying concentrations (Figure 2), and even **9** was not soluble above 100 μ M, limiting accurate determination of EC₅₀. Thus, substituting Ser by isoxazolyl and Ile by Cha had converted Ser-Leu-Ile-NH₂ into a small molecule agonist **9** (MW 378) of comparable potency to, but half the size of, the hexapeptide SLIGRL-NH₂ (MW 657).



Derivatization of Agonist 9. Linking an amine to **9** in order to mimic the arginine side-chain in SLIGRL-NH₂ was considered to be a worthwhile interim measure for both enhancing agonist potency and increasing water solubility. Compound **9** was linked to three different amine-containing moieties using one of two aliphatic linkers of different length (Schemes S1–S3, Supporting Information). Either 1,3-diaminopropane or 1,5-diaminopentane was coupled to TCP

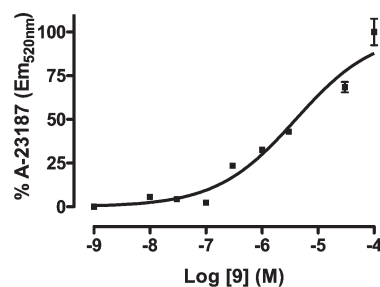


Figure 2. Concentration dependent iCa²⁺ release in HEK293 cells by compound **9**, expressed as % response induced by ionophore A-23187.

Table 2. Effect of C-Terminal Substituent R in **11–18** on Agonist-Induced Calcium Mobilization in HT29 Cells

Chemical structure of the general scaffold for compounds **11–18**. It features a piperidine ring with a carbonyl group and a chain of amino acids (Ser, Leu, Ile) ending in a substituent R.

Compound	n	R	% Response ¹
11	2	(CH ₂) ₂ NH ₂	57
12	4	(CH ₂) ₄ NH ₂	60
13	2	(CH ₂) ₂ NHCO	97
14	4	(CH ₂) ₄ NHCO	181
15	2	(CH ₂) ₂ NHCO	122
16	4	(CH ₂) ₄ NHCO	130
17	2	(CH ₂) ₂ NHCO	130
18	4	(CH ₂) ₄ NHCO	142

¹ At 1 μ M relative to 1 μ M SLIGRLI-NH₂ (100% iCa²⁺).

resin, and then isoleucine, cyclohexylalanine, and isoxazole-5-carboxylic acid were sequentially coupled to each diamine via standard Fmoc chemistry (Scheme S1, Supporting Information). Similarly, 4-(aminomethyl)piperidine and 4-(2-aminoethyl)aniline were separately coupled to TCP resin in parallel, the resins were split two more times, and each functional group was coupled to either the Fmoc-5-aminovaleric acid or Fmoc- β -alanine linkers, followed by the sequential coupling of the remaining amino acids (Scheme S2, Supporting Information). Finally, the use of a pyridine moiety as a functional group necessitated commencing the solid phase synthesis by coupling the linkers to TCP resin (Scheme S3, Supporting Information). Either Fmoc-protected 5-aminovaleric acid or Fmoc- β -alanine was first coupled to TCP resin. Ile, Cha and isoxazole were then sequentially coupled to the linkers via Fmoc SPPS and then cleaved and purified by rpHPLC. The two intermediates were then amidated with 3-aminomethyl pyridine via the free acid to give compounds **11–18** (Table 2).

Compounds **11–18** were more water-soluble than **5** or **9**. Compared with SLIGRLI-NH₂,^{63,64} all were more effective agonists at 1 μ M in eliciting iCa²⁺ release in HT29 cells (Table 2). Agonist potency improved over the more flexible analogues (**11**, **12**) when the amine was mounted on a more constrained linker (e.g., **13–16**) that restricts conformational freedom, possibly directing the amine to a hydrogen bond acceptor in PAR2. Alternatively, the cyclic group may provide additional hydrophobic interactions with PAR2. Terminating the ligand with a pyridine substituent (**15**, **16**), capable of aromatic, hydrophobic, or ionic interactions with receptor, was also beneficial for agonist potency. In all cases,

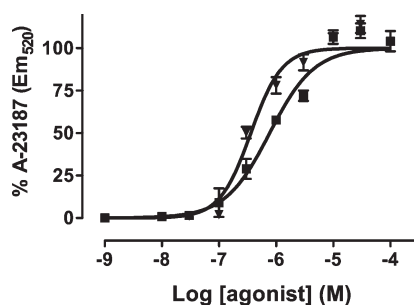


Figure 3. Ca²⁺ release in HT29 cells for **14** (▼) versus SLIGRLI-NH₂ (■), relative to 100% for A-23187 (mean \pm SEM).

increasing the distance between the component analogous to **9** and the amine terminus was advantageous, especially for **13** and **14**. Whilst coupling the 4-(aminomethyl)piperidine moiety to the lead with the shorter β -alanine (**13**) elicited a 97% response, extending the same ligand via 5-aminovaleric acid (**14**) elicited an even stronger calcium response (181% of that for SLIGRLI-NH₂). A full concentration–response curve for agonist **14** in HEK293 cells gave EC₅₀ 0.37 μ M (Figure 3).

To further improve agonist potency, a set of more constrained linkers was examined in place of the flexible ethylenediamine linker in **14** while still enabling flexible orienting and favorable positioning of the amine in the receptor. Compounds **19–28** were obtained through parallel synthesis by first coupling 4-(aminomethyl)piperidine to TCP resin and then protecting the primary amine with 1,3-dimethyl-5-[(dimethylamino)methylene]-2,4,6-(1H,3H,5H)-trioxopyrimidine (DTPM) (Scheme S4, Supporting Information). This allowed the analogues to be synthesized in parallel, while reducing side-product formed when the 4-(aminomethyl)piperidine was coupled to the linker via the secondary amine. The relatively low reactivity of the linker amine resulted in some side products in which the adjoining isoleucine residue had racemized, as well as deletion products in which the isoleucine failed to couple to the linker. These impurities were readily separated from the product by

Table 3. Release of iCa²⁺ in HT29 Cells by Constrained PAR2 Agonists **19–28**

	R	pEC ₅₀ (n, EC ₅₀)	R	pEC ₅₀ (n, EC ₅₀)
19		6.6 \pm 0.02 (4, 0.28 μ M)	24	4.8 \pm 0.05 (3, 17.1 μ M)
20		4.9 \pm 0.03 (3, 13.7 μ M)	25	5.7 \pm 0.1 (2, 2.2 μ M)
21		> 4.3 (2, >50 μ M)	26	5.1 \pm 0.05 (2, 7.1 μ M)
22		6.5 \pm 0.05 (4, 0.34 μ M)	27	5.2 \pm 0.04 (2, 6.1 μ M)
23		6.0 \pm 0.1 (4, 1.1 μ M)	28	4.9 \pm 0.05 (3, 13.5 μ M)

rpHPLC. Larger scale preparations of potent ligands were made in solution using Boc-protected amino acids and linkers, starting from DTPM-protected 4-aminomethylpiperidine with deprotection at the end of the synthesis using 2% hydrazine in DMF. Solution phase chemistry eliminated racemization of the isoleucine residue. Agonist activity was measured for compounds **19**–**28** by calcium efflux in HT29 human colon carcinoma cells (Table 3).

Restricting the conformational freedom of the linker with a 4-(aminomethyl)piperidine- substituent in **19** was slightly more effective than the aminobutyl- linker of **14** (EC_{50} 0.28 vs 0.36 μ M). However, coupling of the tightly constrained aminomethyl piperidine moiety *para* to the isoleucine carbonyl via an isonipecotic acid linker (**20**) proved to be detrimental for agonist activity. Coupling the two functional groups *para* to each other, but altering the length and conformation with a phenyl linker (4-aminobenzoic acid, **21**), further reduced potency. Addition of a methylene group to the linker, adding some flexibility to the scaffold, was beneficial for activity of the *para* coupled linkers, more so when the methylene was situated between the phenyl ring and the aminomethyl piperidine group using 4-aminophenylacetic acid (**22**) than when before the linker via 4-aminomethylbenzoic acid (**23**). Similar observations were noted when *meta*-coupling linkers were employed. While substitution with the aliphatic nipectic acid linker (**24**) decreased potency of the ligand \sim 45-fold, substitution with 3-aminobenzoic acid (**25**) resulted in agonist activity comparable to that of SLIGRL-NH₂, however still less potent than the valeric acid-linked agonist. Extending the compound by adding a methylene with 3-aminomethylbenzoic acid was beneficial, resulting in the most potent ligand of this series (**19**, EC_{50} 0.28 ± 0.01 μ M). Enforcing a rigid turn conformation, either an α -turn via the pipecolic acid linker (**26**) or a β -turn with a dipeptide (**27**) or Freidinger's lactam (**28**) linkers, was not conducive for agonist activity. Thus, incorporating constraints in **14** improved agonist potency, provided that the linker was not too rigid and that there was some degree of flexibility, perhaps enabling the amine to make a key interaction with receptor residues.

Next, the selectivity for PAR2 over PAR1 of the most potent compounds from the constrained agonist library was evaluated via a desensitization assay (Figure 4). As described above, HT29 cells were administered with 2f-LIGRLI-NH₂ (6.7 μ M) at t_0 and then re-exposed at t_{300} to a second treatment of the same compound (7.5 μ M). This second addition of PAR2 agonist failed to generate calcium efflux, indicating that cells had been desensitized to PAR2 activation (Figure 4A). Following desensitization via exposure to 2f-LIGRLI-NH₂, cells were treated at t_{300} with 100 μ M **19** (Figure 4B). This also failed to generate a calcium response, suggesting that **19** is acting via the PAR2 receptor. Treating cells with **22** at t_{300} after first desensitizing with 2f-LIGRLI-NH₂ (Figure 4C) did generate a calcium response, indicating that agonist **22** was not selective for PAR2 and thus it is likely activating other receptors.

Serum Stability of PAR2 Agonists 19 and 29. To assess whether reducing the peptidic content of the PAR2 agonist improved serum stability, resistance to proteolysis was compared for (a) SLIGRL-NH₂, (b) 4-(2-methyloxazolyl)-LIGR-(4-I)Phe-NH₂ (**29**) containing a heterocyclic moiety in place of serine and the unnatural amino acid 4-iodophenylalanine in place of leucine, and (c) compound **19**. Compound **29** has previously been reported by us (compound 52

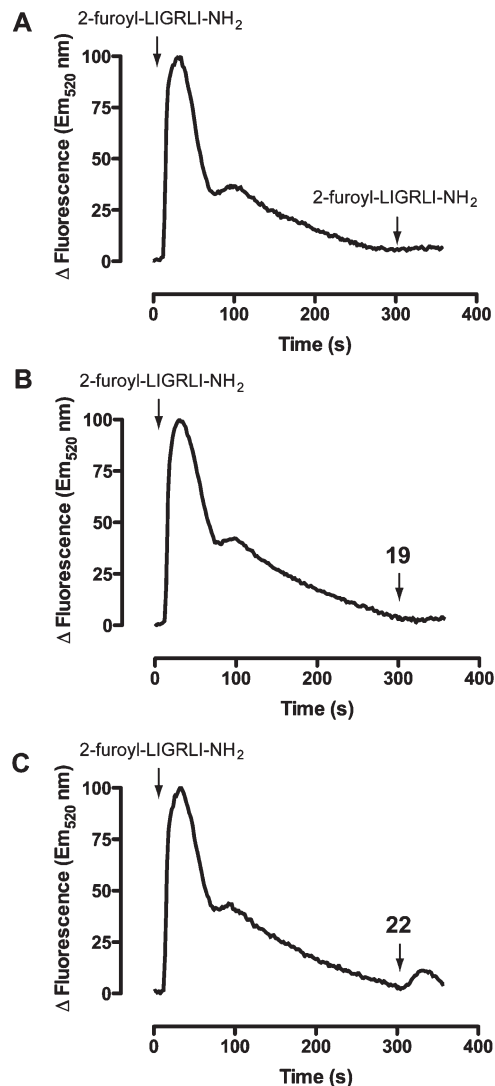


Figure 4. Desensitization assays for constrained PAR2 agonists. (A) Control using 2-furoyl-LIGRLI-NH₂ at t_0 to desensitize PAR2 on HT29 cells, then treated at t_{300} with 2-furoyl-LIGRLI-NH₂ (6.7 μ M) to demonstrate PAR2 desensitization. (B) Cells treated with 2-furoyl-LIGRLI-NH₂ at t_0 and then at t_{300} with compound **19** (100 μ M). (C) After desensitizing cells with 2-furoyl-LIGRLI-NH₂, compound **22** (100 μ M) was administered at t_{300} . Thus, agonist **19** is PAR2 selective, and **22** is not PAR2 selective.

in ref 64) and is one of the most potent and serum-stable peptide agonists reported to date. Each compound was added to filtered fetal calf serum (5 mL) so that the final concentration of agonist was 1 mM. At regular intervals, 500 μ L aliquots were removed and added to 1.5 mL MeCN. The solution was centrifuged (2500 rpm, 5 min) before removing supernatant (1 mL) and analyzing via ESMS and rpHPLC. Data from these experiments are expressed as percent of peak area recorded from the HPLC trace at t_0 (Figure 5). Over 95% **19** was present in FCS after 4 h, compared with \sim 78% **29** and 57% SLIGRL-NH₂. In addition to serum stability, compound **19** has cLogP 3.1, 4 H-bond donors, and 7 H-bond acceptors, and it conforms to Lipinski's rule of five with the exception of molecular weight (608.8). These properties have enabled ongoing studies in experimental pharmacology with **19** in animal models of inflammatory diseases. The potency, selectivity, serum stability, and druglike composition of **19** makes it more

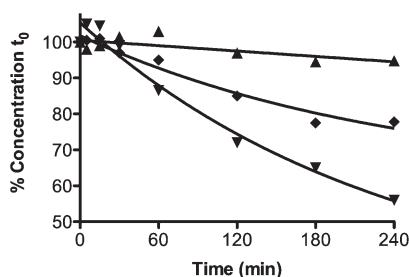
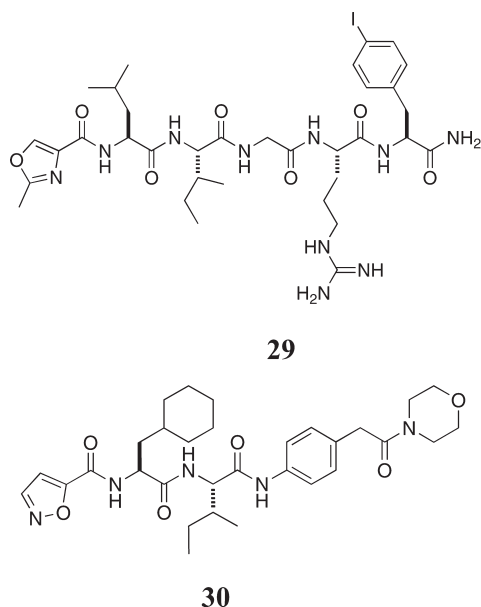


Figure 5. Comparative serum stability of PAR2 agonists SLIGRL-NH₂ (▼), **19** (▲), and **29** (◆) in FCS at 37 °C over 4 h. Data expressed as percent of peak area from HPLC trace at $t = 0$.

effective than known PAR2 agonists and should enable its use as an effective probe of the biological functions of PAR2 in vivo.



Conversion to PAR2 Antagonists 30, 35, and 36. Based on the PAR2 agonist activity of compound **22**, we decided to probe the importance of the primary amine substituent appended to the piperidine group, without substantially altering the space-filling characteristics of **22**. Replacing the aminomethyl piperidine moiety with morpholine gave compound **30**. In contrast to the agonist profile shown by **19** on HT29 cells (Figure 6A), compound **30** showed no agonist activity but did inhibit intracellular Ca²⁺ release induced by 2.5 μM SLIGRLI-NH₂ (Figure 6B). The inhibition assay was performed by preincubating HT29 cells with increasing concentrations of **30** 15 min prior to administration of SLIGRLI-NH₂ at 2.5 μM (EC₈₀). Although not a potent antagonist (IC₅₀ 57 μM), this was a clue for the design and development of PAR2 antagonists.

The steric effect on antagonist potency was examined by appending bulky uncharged moieties directly to the agonist template **9**, amidating with different amines bearing bi and tricyclic fused rings that could interrogate different pharmacophore space. These included tetrahydroisoquinoline (**31**), 1-naphthylamine (**32**), *N*-phenylpiperazine (**33**, **34**), 2-aminobiphenyl (**35**), and spiroindanepiperidine (**36**) (Figure 7). Antagonist activity was assessed in single point inhibition assays at 5 and 50 μM concentrations against 2.5 μM SLIGRLI-NH₂ (Figure 7A). At 5 μM, these compounds attenuated the agonist response of SLIGRLI-NH₂ by

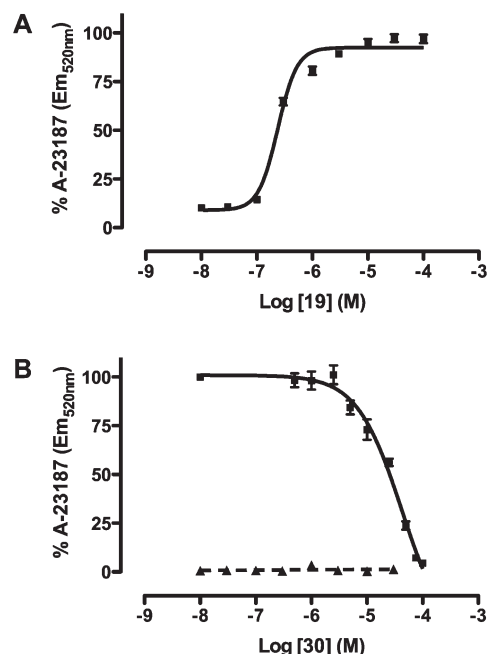


Figure 6. Comparison of iCa²⁺ release in HT29 cells. (A) PAR2 agonist **19** (EC₅₀ 0.34 ± 0.05 μM). (B) PAR2 antagonist **30** alone (▲) or its inhibition of 2.5 μM agonist SLIGRLI-NH₂ (■, IC₅₀ 57 μM). Data = mean ± SEM ($n = 3$).

40–80%, and at 50 μM compound **36** completely inhibited the intracellular calcium efflux. To determine if the observed inhibition could be attributed to PAR2 desensitization, the compounds were also evaluated alone for agonist activity at 50 μM concentrations (Figure 7B). Compounds **31**, **33**, and **34** were clearly weak agonists, eliciting a calcium efflux greater than that observed for 2.5 μM SLIGRLI-NH₂. Compound **32** appeared to have little activity toward PAR2, as either an agonist or antagonist. Compounds **35** and **36** showed negligible agonist activity as defined by Ca²⁺ release in HT29 cells, and thus, they can be confidently assigned as antagonists of PAR2 on these cells. Compound **36** was the more potent antagonist in full concentration–response curves (2 μM ± 1.0 μM, Figure 8).

Figure 8A compares intracellular Ca²⁺ release induced in HT29 colon carcinoma cells by three different PAR2 agonists, demonstrating with concentration response curves that agonist **19** (■, pEC₅₀ 6.6 ± 0.05) is an equipotent agonist with hexapeptide 2f-LIGRLO-NH₂ (○, pEC₅₀ 6.7 ± 0.05), but it is not as potent as trypsin (pEC₅₀ 8.2 ± 0.08). Compound **19** was also selective (up to 100 μM) for PAR2 over PAR1, as indicated by lack of response after PAR2 was desensitized by 5 μM 2f-LIGRLO-NH₂ (Figure 4B).

Figure 8B shows that antagonist **36** selectively inhibited iCa²⁺ release induced in HT29 cells by two different PAR2 agonists at their EC₈₀ concentrations: trypsin (pIC₅₀ 5.7 ± 0.1) and 2f-LIGRLO-NH₂ (pIC₅₀ 5.1 ± 0.2). It also antagonizes **19** (pIC₅₀ 5.1 ± 0.2; data not shown). Moreover, **36** had no effect against PAR1 agonist thrombin at 10 U/mL. Compound **36** is the only PAR2 antagonist reported to date that is able to inhibit at low micromolar concentrations both trypsin- and peptide-agonist-induced iCa²⁺ in PAR2 expressing native cells, with others being either several orders of magnitude less potent⁵⁴ or unable to block endogenous protease agonists of PAR2.⁵⁵ The present data support the idea that the nonpeptidic PAR2-selective agonist **19** and

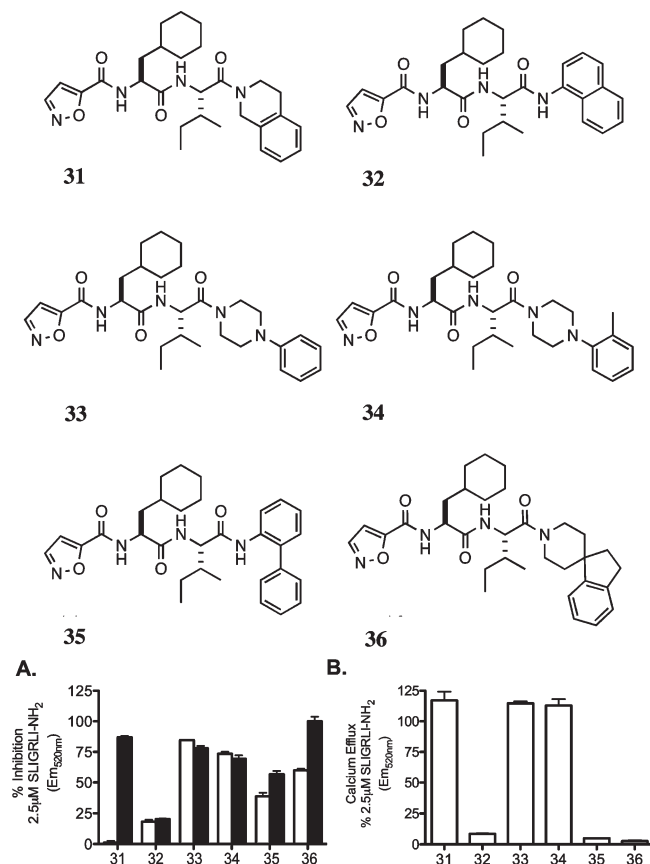


Figure 7. Prospective PAR2 antagonists (31–36). (A) Compounds 31–36 tested for antagonism at 5 μM (clear) and 50 μM (black) by inhibition of calcium efflux elicited in HT29 cells by SLIGRLI-NH₂ (2.5 μM). Each column represents percent inhibition versus 100% for complete inhibition. (B) Compounds 31–36 tested at 50 μM for agonist activity (% calcium efflux relative to 100% for SLIGRLI-NH₂ at 2.5 μM). Compounds 35 and 36 are antagonists.

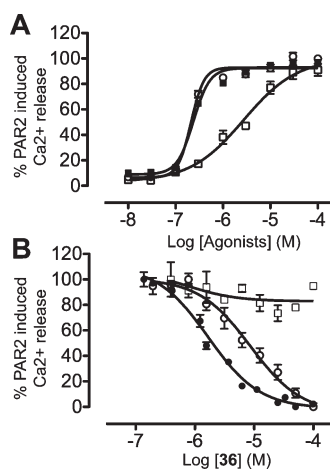


Figure 8. Characterization of nonpeptide agonist GB110 (19) and antagonist GB83 (36) of PAR2. (A) Comparison of PAR2 agonist-induced intracellular Ca²⁺ release in HT29 colon carcinoma cells by hexapeptide SLIGRL-NH₂ (□, pEC₅₀ 5.6 ± 0.15), hexapeptide 2f-LIGRLO-NH₂ (○, pEC₅₀ 6.7 ± 0.05), and 19 (■, pEC₅₀ 6.6 ± 0.05). 19 is equipotent with one of the most potent known PAR2 activating peptides, 2f-LIGRLO-NH₂. (B) 36 selectively inhibits intracellular Ca²⁺ release induced in HT29 cells by two different PAR2 agonists at their EC₈₀ concentrations: trypsin (●, pIC₅₀ 5.7 ± 0.1) and 2f-LIGRLO-NH₂ (○, pIC₅₀ 5.1 ± 0.2). But it has no effect against PAR1 agonist thrombin (□) at 10U/mL.

antagonist 36 could be extremely valuable tools for probing PAR2 activation and blockade in vivo.

Conclusions. The G protein coupled receptor known as protease activated receptor 2 (PAR2) is upregulated in many inflammatory diseases and multiple cancers. It is activated in vivo by mainly serine proteases (e.g. trypsin, tryptase), which cleave the N-terminus of the receptor, but there are no known nonproteolytic endogenous agonists. Although short synthetic peptides, corresponding to the new PAR2 N-terminus created through cleavage, are weak PAR2 agonists, they are mainly of low potency, questionable selectivity, and poor bioavailability that limit their usefulness and reliability as PAR2 investigative tools in vivo. Here we have derived short agonist peptides, converted them to more potent PAR2 agonists by replacing amino acids with certain nonpeptidic fragments often present in other GPCR ligands,¹ and derived nonpeptidic PAR2 antagonists through structure–activity relationships. Nonpeptidic agonist 19 (EC₅₀ 280 nM) selectively induced intracellular Ca²⁺ release in human colorectal carcinoma cells with comparable potency to the most potent known peptide agonist 2f-LIGRLO-NH₂. Nonpeptidic antagonist 36 (IC₅₀ 2 μM) selectively and reversibly inhibits intracellular Ca²⁺ release induced in HT29 cells by three different PAR2 agonists (trypsin, 2f-LIGRLO-NH₂, and 19), and it does not inhibit the PAR1 agonist thrombin. Compound 36 is the most potent and only known PAR2 antagonist reported to inhibit both trypsin- and peptide-induced activation of PAR2 at low micromolar concentrations. PAR2 agonist 19 will be designated GB110 and PAR2 antagonist 36 will be GB83 in future reports by our group on in vivo properties of these compounds. Compounds 19 and 36, which were selective for PAR2 over PAR1 with no effect on intracellular Ca²⁺ release in cells desensitized to PAR2 activation, are serum stable and suitable for oral administration, thus enabling pharmacological investigation of the effects of PAR2 regulation in animal models of human diseases.

Experimental Methods

Compounds 1–7. Portions (7 × 200 mg) of rink amide MBHA resin (0.14 mmol scale) were sequentially coupled with two Fmoc-protected amino acids (4 equiv amino acid, 4 equiv HBTU, 4 equiv DIPEA, in DMF), followed by furan-2-carboxylic acid (4 equiv HBTU, 4 equiv DIPEA, in DMF), following standard Fmoc SPPS. Ligands were then cleaved from resin using 95:2.5:2.5 TFA/TIPS/H₂O stirred for 1.5 h. The solvent was filtered in a sintered glass funnel and then removed in vacuo, and products were purified via rpHPLC fitted with a tunable absorbance detector (λ 214 nm), using a Phenomenex C18 column (300 Å, 22 × 250 mm) with a gradient of 0% B to 100% B over 30 min (solvent A 0.1% TFA in H₂O, solvent B 0.1% TFA, 10% acetonitrile, 90% H₂O). Compounds were characterized by HRMS, compounds were characterized by HRMS and ¹H NMR using DMSO-*d*₆ as solvent, and purity of compounds was assessed via analytical rpHPLC under different conditions (0% B to 100% B over 30 min gradient, Phenomenex C18 column, 300 Å, 4.6 × 250 mm, 214 nm λ). Compounds were repurified if found to be below 95%, with all final compounds being >95% pure by analytical HPLC trace analysis.

2-Furoyl-Leu-Ile-NH₂ (1). Yield 15 mg (28% isolated); R_t 22.24 min; HRMS 338.2074 (calc), 338.2068 (found). ¹H NMR (400 MHz), δ 0.81 (t, 5H, J = 6.90 Hz); 0.82 (d, 6H, J = 6.90 Hz); 0.85 (d, 3H, J = 6.43 Hz); 0.89 (d, 3H, J = 6.37 Hz); 1.01–1.09 (m, 1H); 1.39–1.53 (m, 2H); 1.59–1.72 (m, 3H); 4.13 (dd, 1H, J 7.30, 8.98 Hz); 4.46–4.52 (m 1H); 6.63 (q, 1H); 7.00 (s 1H); 7.18 (dd, 1H, J = 0.82, 3.48 Hz); 7.38 (s, 1H); 7.72 (d, 1H, J = 9.02 Hz); 7.86 (dd, 1H, J = 0.81, 1.75 Hz); 8.33 (d, 1H, J = 8.48 Hz).

2-Furoyl-Leu-Cha-NH₂ (2). Yield 26 mg (49% isolated); *R_t* 25.38 min; HRMS 378.2387 (calc), 378.2394 (found). ¹H NMR (400 MHz), δ 0.86 (d, 4H, *J* = 6.32 Hz); 0.90 (d, 4H, *J* = 6.24 Hz); 1.11–1.20 (m, 3H); 1.29–1.43 (m, 1H); 1.43–1.68 (m 10H); 4.25–4.28 (m, 1H); 4.41–4.47 (m, 1H); 6.63 (q, 1H); 6.95 (s 1H); 7.18 (dd, 1H, *J* = 0.78, 3.49 Hz); 7.24 (s, 1H); 7.84–7.86 (m, 2H); 8.30 (d, 1H, *J* = 8.30 Hz).

2-Furoyl-Leu-Phe-NH₂ (3). Yield 10 mg (19% isolated); *R_t* 23.34 min; HRMS 372.1918 (calc), 372.1924 (found). ¹H NMR (400 MHz), δ 0.81 (d, 3H, *J* = 6.43 Hz); 0.85 (d, 3H, *J* = 6.38 Hz); 1.37–1.42 (m, 1H); 1.48–1.59 (m, 2H); 2.81 (dd, 1H, *J* = 9.03, 13.84 Hz); 3.00 (dd, 1H, *J* = 4.95, 13.78 Hz); 4.36–4.46 (m, 2H); 6.64 (q, 1H); 7.07 (s, 1H); 7.17–7.19 (m, 5H); 7.36 (s, 1H); 7.86 (dd, 1H, *J* = 0.81, 1.75 Hz); 7.92 (d, 1H, *J* = 8.41 Hz); 8.25 (d, 1H, *J* = 8.26 Hz).

2-Furoyl-Leu-(p-F)Phe-NH₂ (4). Yield 15 mg (27% isolated); *R_t* 23.87 min; HRMS 390.1824 (calc), 390.1812 (found). ¹H NMR (400 MHz), δ 0.81 (d, 3H, *J* = 6.43 Hz); 0.86 (d, 3H, *J* = 6.37 Hz); 1.35–1.41 (m, 1H); 1.45–1.59 (m, 2H); 2.79 (dd, 1H, *J* = 9.24, 13.65 Hz); 2.99 (dd, 1H, *J* = 5.07, 13.98 Hz); 4.35–4.45 (m, 2H); 6.64 (q, 1H); 6.96–7.00 (m, 2H); 7.09 (s, 1H); 7.18 (dd, 1H, *J* = 0.81, 3.49 Hz); 7.21 (dd, 2H, *J* = 5.63, 8.72 Hz); 7.39 (s, 1H); 7.86 (dd, 1H, *J* = 0.82, 1.75 Hz); 7.92 (d, 1H, *J* = 8.45 Hz); 8.24 (d, 1H, *J* = 8.20 Hz).

2-Furoyl-Cha-Ile-NH₂ (5). Yield 26 mg (49% isolated); *R_t* 25.11 min; HRMS 378.2387 (calc), 378.2375 (found). ¹H NMR (400 MHz), δ 0.80 (t, 7H, 6.90 Hz); 0.81 (d, 5H, 6.90 Hz); 1.00–1.15 (m, 3H); 1.24–1.34 (m, 1H); 1.37–1.45 (m, 1H); 1.50–1.72 (m, 8H); 4.12 (dd, 1H, *J* = 7.39, 9.02 Hz); 4.48–4.54 (m, 1H); 6.63 (q, 1H); 7.01 (s, 1H); 7.18 (dd, 1H, *J* = 0.84, 3.46 Hz); 7.37 (s, 1H); 7.71 (d, 1H, *J* = 8.91 Hz); 7.86 (dd, 1H, *J* = 0.83, 1.75 Hz); 8.31 (d, 1H, *J* = 8.43 Hz).

2-Furoyl-Phe-Ile-NH₂ (6). Yield 13 mg (25% isolated); *R_t* 22.61 min; HRMS 372.1918 (calc), 372.1927 (found). ¹H NMR (400 MHz), δ 0.80–0.85 (m, 7H); 1.02–1.11 (m, 1H); 1.39–1.48 (m, 1H); 1.68–1.75 (m, 1H); 2.96 (dd, 1H, *J* = 11.11, 10.36 Hz); 3.08 (dd, 1H, *J* = 4.18, 14.39 Hz); 4.17 (dd, 1H, *J* = 7.14, 9.05 Hz); 4.70–4.76 (m, 1H); 7.04 (s, 1H); 7.10 (d, 1H, *J* = 4.04 Hz); 7.15 (t, 1H, *J* = 7.23 Hz); 7.23 (t, 2H, *J* = 7.31 Hz); 7.30 (d, 1H, *J* = 8.41 Hz); 7.38 (s, 1H); 7.82 (d, 1H, *J* = 1.66 Hz); 7.93 (d, 1H, *J* = 9.04 Hz); 8.34 (d, 1H, *J* = 8.67 Hz).

2-Furoyl-Chg-Ile-NH₂ (7). Yield 3 mg (6% isolated); *R_t* 23.15 min; HRMS 364.2231 (calc), 364.2243 (found). ¹H NMR (400 MHz), δ 0.79–0.83 (m, 8H); 1.00–1.09 (m, 1H); 1.37–1.45 (m, 1H); 1.65–1.70 (m, 1H); 2.96 (dd, 1H, *J* = 11.11, 10.36 Hz); 4.12 (dd, 1H, *J* = 8.14, 9.04 Hz); 4.332 (t, 1H, *J* = 8.43 Hz); 6.63 (q, 1H); 6.70 (s, 1H); 7.19 (dd, 1H, *J* = 0.80, 3.47 Hz); 7.33 (s, 1H); 7.85 (dd, 1H, *J* = 0.80, 1.75 Hz); 7.88 (d, 1H, *J* = 8.88 Hz); 8.01 (d, 1H, *J* = 8.90 Hz).

Compounds 8–10. Portions (6 × 200 mg) of rink amide MBHA resin (0.14 mmol scale) were sequentially coupled with Fmoc-Ile-OH (4 equiv) and then either Fmoc-Leu-OH or Fmoc-Cha-OH in a solution consisting of HBTU (4 equiv) and DIPEA (4 equiv) in DMF (2 mL). Upon completion, compounds were coupled with either pyrazine-2-carboxylic acid, isoxazole-5-carboxylic acid, or 2-methyloxazole-4-carboxylic acid (all 4 equiv) in the presence of HBTU (4 equiv), and of DIPEA (4 equiv) in DMF (2 mL). Ligands were then cleaved from resin using 95:2.5:2.5 TFA/TIPS/H₂O, solvent was removed in vacuo, and products were purified via rpHPLC fitted with a tunable absorbance detector (214 nm λ), using a Phenomenex C18 column (300 Å, 22 × 250 mm) with a gradient of 0% B to 100% B over 30 min (solvent A 0.1% TFA in H₂O, solvent B 0.1% TFA, 10% acetonitrile, 90% H₂O). Compounds were characterized by HRMS and ¹H NMR using DMSO-*d*₆ as solvent, and purity of compounds was assessed via analytical rpHPLC (0% B to 100% B over 30 min gradient, Phenomenex C18 column, 300 Å, 4.6 × 250 mm, λ 214 nm). Compounds were repurified if found to be below 95%.

2-Pyrazoyl-Leu-Ile-NH₂. Yield 5 mg (10% isolated); *R_t* 21.23 min; HRMS 350.2187 (calc), 350.2199 (found). ¹H NMR (400

MHz), δ 0.79–0.83 (m, 7H); 0.889 (d, 7H, *J* = 5.74 Hz); 1.02–1.10 (m, 1H); 1.37–1.45 (m, 1H); 1.52–1.61 (m, 2H); 1.67–1.72 (m, 2H); 4.152 (dd, 1H, *J* = 7.46, 8.94 Hz); 4.62–4.68 (m, 1H); 6.997 (s, 1H); 7.405 (s, 1H); 7.984 (d, 1H, *J* = 8.97 Hz); 8.770 (dd, 1H, *J* = 1.53, 2.52 Hz); 8.807 (d, 1H, *J* = 8.98 Hz); 8.903 (d, 1H, *J* = 2.39 Hz); 9.190 (d, 1H, *J* = 1.43 Hz).

2-Pyrazoyl-Cha-Ile-NH₂ (8). Yield 30 mg (55% isolated); *R_t* 24.46 min; HRMS 390.2500 (calc), 390.2514 (found). ¹H NMR (400 MHz), δ 0.79–0.83 (m, 8H); 0.85–0.94 (m, 2H); 1.02–1.17 (m, 5H); 1.23–1.30 (m, 1H); 1.37–1.46 (m, 1H); 1.55–1.70 (m, 8H); 4.15 (dd, 1H, *J* = 7.47, 8.90 Hz); 4.64–4.70 (m, 1H); 7.00 (s, 1H); 7.40 (s, 1H); 7.99 (d, 1H, *J* = 12.74 Hz); 8.77 (dd, 1H, *J* = 1.48, 2.50 Hz); 8.90 (d, 1H, *J* = 2.42 Hz); 9.19 (d, 1H, *J* = 1.55 Hz).

5-Isoxazolyl-Leu-Ile-NH₂. Yield 8 mg (17% isolated); *R_t* 21.17 min; HRMS 339.2027 (calc), 339.2037 (found). ¹H NMR (400 MHz), δ 0.81 (t, 5H, *J* = 7.62 Hz); 0.82 (d, 4H, *J* = 7.49 Hz); 0.86 (d, 3H, *J* = 6.42 Hz); 0.90 (d, 3H, *J* = 6.38 Hz); 1.00–1.10 (m, 1H); 1.40–1.54 (m, 2H); 1.58–1.73 (m, 3H); 4.13 (dd, 1H, *J* = 7.40, 8.98 Hz); 4.50–4.56 (m 1H); 7.00 (s, 1H); 7.15 (d, 1H, *J* = 1.88 Hz); 7.83 (d, 1H, *J* = 8.98 Hz); 8.75 (d, 1H, *J* = 1.92 Hz); 8.96 (d, 1H, *J* = 8.47 Hz).

5-Isoxazolyl-Cha-Ile-NH₂ (9). Yield 18 mg (34% isolated); *R_t* 24.09 min; HRMS 379.2340 (calc), 379.2351 (found). ¹H NMR (400 MHz), δ 0.79–0.83 (m, 7H); 0.86–0.95 (m, 2H); 1.00–1.19 (m, 4H); 1.26–1.35 (m, 1H); 1.38–1.46 (m, 1H); 1.51–1.72 (m, 8H); 4.12 (dd, 1H, *J* = 7.36, 8.97 Hz); 4.52–4.57 (m, 1H); 7.01 (s, 1H); 7.15 (d, 1H, *J* = 1.91 Hz); 7.37 (s, 1H); 7.82 (d, 1H, *J* = 11.81 Hz); 8.75 (d, 1H, *J* = 1.88 Hz); 8.97 (d, 1H, *J* = 8.18 Hz).

4-(2-Methyloxazolyl)-Leu-Ile-NH₂. Yield 16 mg (32% isolated); *R_t* 21.67 min; HRMS 353.2183 (calc), 353.2196 (found). ¹H NMR (400 MHz), δ 0.811 (t, 7H, *J* = 7.50 Hz); 0.841 (d, 3H, *J* = 9.68 Hz); 0.877 (d, 4H, *J* = 6.50 Hz); 1.02–1.09 (m, 1H); 1.38–1.71 (m, 5H); 4.146 (dd, 1H, *J* = 7.34, 9.01 Hz); 4.51–4.57 (m 1H); 6.994 (s, 1H); 7.405 (s, 1H); 7.881 (d, 1H, *J* = 9.02 Hz); 8.112 (d, 1H, *J* = 8.90 Hz); 8.487 (s, 1H).

4-(2-Methyloxazolyl)-Cha-Ile-NH₂ (10). Yield 23 mg (42% isolated); *R_t* 24.60 min; HRMS 393.2496 (calc), 393.2509 (found). ¹H NMR (400 MHz), δ 0.79–0.90 (m, 8H); 1.02–1.14 (m, 4H); 1.19–1.27 (m, 1H); 1.36–1.44 (m, 1H); 1.48–1.75 (m, 9H); 4.14 (dd, 1H, *J* = 7.42, 8.95 Hz); 4.53–4.59 (m, 1H); 6.99 (s, 1H); 7.39 (s, 1H); 7.881 (d, 1H, *J* = 9.08 Hz); 8.08 (d, 1H, *J* = 8.92 Hz); 8.49 (s, 1H).

Compounds 11 and 12. 1,5-Diaminopentane · 2 HCl (800 mg, 4.6 mmol) was dissolved in a solution of KOH (516 mg, 2 equiv) in MeOH (4 mL) and allowed to stir at rt for 10 min, at which time the KCl salt had precipitated out. The solution was then filtered in a sintered glass funnel and washed with DCM before the solvent was removed in vacuo. Two portions of TCP resin (200 mg, substitution 0.9 mmol · g⁻¹) were reacted with either 1,5-diaminopentane (74 mg, 4 equiv) or 1,3-diaminopropane (53 mg, 4 equiv) dissolved in anhydrous DCM and allowed to shake overnight. Compounds were sequentially coupled with Fmoc-Ile-OH (2 equiv), Fmoc-Cha-OH (2 equiv), and isoxazole-5-carboxylic acid (2 equiv) in the presence of HOBT (4 equiv), DIC (2 equiv), and DIPEA (2 equiv) in DMF (2 mL). The products were cleaved from the resin by treatment with a solution of 20% TFA and 2.5% TIPS in DCM 5 (mL) for 1.5 h and then filtered in a sintered glass funnel before the filtrate was removed in vacuo. Products were isolated by rpHPLC fitted with a tunable absorbance detector (λ 214 nm), using a Phenomenex C18 column (300 Å, 22 × 250 mm) with a gradient of 0% B to 100% B over 30 min (solvent A 0.1% TFA in H₂O, solvent B 0.1% TFA, 10% acetonitrile, 90% H₂O). Compounds were characterized by HRMS and ¹H NMR using DMSO-*d*₆ as solvent, and purity of compounds was assessed via analytical rpHPLC (0% B to 100% B over 30 min gradient, Phenomenex C18 column, 300 Å, 4.6 × 250 mm, 214 nm λ). Compounds were repurified if found to be below 95%.

5-Isoxazolyl-Cha-Ile-amino-3-aminopropane (11). R_t 21.16 min; HRMS 436.2918 (calc), 436.2929 (found). $^1\text{H NMR}$ (400 MHz), δ 0.79–0.83 (m, 7H); 0.85–0.95 (m, 2H); 1.03–1.16 (m, 5H); 1.27–1.34 (m, 1H); 1.38–1.46 (m, 1H); 1.51–1.70 (m, 12H); 2.77 (t, 2H, $J = 7.73$ Hz); 3.00–3.09 (m, 1H); 3.13–3.22 (m, 1H); 4.09 (t, 1H, $J = 8.28$ Hz); 4.51–4.57 (m, 1H); 7.16 (d, 1H, $J = 1.88$ Hz); 7.70 (s, 3H); 7.93 (d, 1H, $J = 13.85$ Hz); 8.13 (t, 1H, $J = 5.68$ Hz); 8.76 (d, 1H, $J = 1.90$ Hz); 8.95 (d, 1H, $J = 8.24$ Hz).

5-Isoxazolyl-Cha-Ile-amino-5-aminopentane (12). R_t 21.74 min; HRMS 464.3231 (calc), 464.3245 (found). $^1\text{H NMR}$ (400 MHz), δ 0.79–0.82 (m, 8H); 0.85–0.95 (m, 2H); 1.02–1.16 (m, 5H); 1.23–1.31 (m, 4H); 1.35–1.44 (m, 4H); 1.47–1.69 (m, 12H); 2.75 (t, 2H, $J = 7.85$ Hz); 2.93–3.01 (m, 1H); 3.05–3.13 (m, 1H); 4.09 (t, 1H, $J = 8.55$ Hz); 4.51–4.57 (m, 1H); 7.15 (d, 1H, $J = 1.89$ Hz); 7.64 (s, 3H); 7.88 (d, 1H, $J = 8.90$ Hz); 7.96 (t, 1H, $J = 5.41$ Hz); 8.76 (d, 1H, $J = 1.91$ Hz); 8.95 (d, 1H, $J = 8.18$ Hz).

Compounds 13 and 14. 4-Aminomethyl piperidine (82 mg, 4 equiv) was dissolved in anhydrous DCM (2 mL) and then added to TCP resin (2×200 mg, substitution $0.9 \text{ mmol} \cdot \text{g}^{-1}$) and shaken overnight. The free amine was then reacted with either Fmoc- β -Ala-OH (2 equiv) or Fmoc-5-aminovaleic acid (2 equiv) and then dissolved in a solution of DCM (2 mL) and DIC (1 equiv). Fmoc-Ile-OH (2 equiv), Fmoc-Cha-OH (2 equiv), and isoxazole-5-carboxylic acid (2 equiv) were then sequentially coupled following standard Fmoc-SPPS, using HOBt (4 equiv) and DIC (2 equiv) to activate the acid and DIPEA (2 equiv) as base dissolved in DMF (2 mL). Upon completion, products were cleaved from the resin by treatment with a solution of 20% TFA and 2.5% TIPS in DCM (5 mL) for 1.5 h. The solution was then filtered in a sintered glass funnel, and the filtrate was removed in vacuo. Crude products were purified by rpHPLC fitted with a tunable absorbance detector (λ 214 nm), using a Phenomenex C18 column (300 Å, 22×250 mm) with a gradient of 0% B to 100% B over 30 min (solvent A 0.1% TFA in H_2O , solvent B 0.1% TFA, 10% acetonitrile, 90% H_2O). Compounds were characterized by HRMS and $^1\text{H NMR}$ using $\text{DMSO-}d_6$ as solvent, and purity of compounds was assessed via analytical rpHPLC (0% B to 100% B over 30 min gradient, Phenomenex C18 column, 300 Å, 4.6×250 mm, 214 nm λ). Compounds were repurified if found to be below 95%.

5-Isoxazolyl-Cha-Ile-amino-(3-(4-aminomethyl)piperidin-1-yl)propan-3-one (13). R_t 21.15 min; HRMS 547.3602 (calc), 547.3617 (found). $^1\text{H NMR}$ (400 MHz), δ 0.77–0.81 (m, 8H); 0.83–0.95 (m, 2H); 1.02–1.13 (m, 5H); 1.34–1.47 (m, 5H); 1.55–1.71 (m, 12H); 1.96–2.01 (m, 1H); 2.11–2.17 (m, 1H); 2.65 (s, 1H); 2.67–2.72 (m, 2H); 3.00–3.08 (m, 1H); 4.06 (t, 1H, $J = 8.09$ Hz); 4.46–4.51 (m, 1H); 7.12 (d, 1H, $J = 1.87$ Hz); 7.719 (s, 2H); 7.85–7.89 (m, 1H); 7.95 (t, 1H, $J = 5.84$ Hz); 8.754 (d, 1H, $J = 1.91$ Hz); 8.960 (d, 1H, $J = 15.84$ Hz).

5-Isoxazolyl-Cha-Ile-amino-[5-(4-aminomethyl)piperidin-1-yl]pentan-5-one (14). R_t 21.49 min; HRMS 575.3915 (calc), 575.3929 (found). $^1\text{H NMR}$ (400 MHz), δ 0.78–0.82 (m, 7H); 0.85–0.91 (m, 2H); 1.03–1.12 (m, 5H); 1.37–1.43 (m, 1H); 1.54–1.75 (m, 12H); 2.04–2.07 (m, 1H); 2.25–2.29 (m, 1H); 2.71 (s, 1H); 2.92–2.98 (m, 2H); 3.06–3.11 (m, 1H); 4.10 (t, 1H, $J = 7.97$ Hz); 4.51–4.57 (m, 1H); 7.15 (d, 1H, $J = 1.87$ Hz); 7.76 (s, 2H); 7.84–7.89 (m, 1H); 7.96 (t, 1H, $J = 5.79$ Hz); 8.75 (d, 1H, $J = 1.91$ Hz); 8.95 (d, 1H, $J = 8.26$ Hz).

Compounds 15 and 16. 4-(2-Aminoethyl) aniline (98 mg, 0.72 mmol), dissolved in anhydrous DCM (2 mL) was added to two portions of TCP resin (200 mg, substitution $0.9 \text{ mmol} \cdot \text{g}^{-1}$) and allowed to shake overnight. The solution was then removed from the resin, and each was coupled with either Fmoc- β -Ala-OH (112 mg, 2 equiv) or Fmoc-5-aminovaleic acid (122 mg, 2 equiv) using DIC (28 μL) in DCM (2 mL) to form an acid anhydride intermediate. Next, Fmoc-Ile-OH (2 equiv), Fmoc-Cha-OH (2 equiv), and isoxazole-5-carboxylic acid (2 equiv) were sequentially coupled following Fmoc SPPS, with HOBt (4 equiv), DIC (2 equiv), and DIPEA (2 equiv) in DMF

(2 mL). Products were then cleaved from the resin by treatment with a solution of 20% TFA and 2.5% TIPS in DCM (5 mL) for 1.5 h. The solution was then filtered in a sintered glass funnel, and the filtrate was removed in vacuo. Crude products were isolated by rpHPLC fitted with a tunable absorbance detector (λ 214 nm), using a Phenomenex C18 column (300 Å, 22×250 mm) with a gradient of 0% B to 100% B over 30 min (solvent A 0.1% TFA in H_2O , solvent B 0.1% TFA, 10% acetonitrile, 90% H_2O). Compounds were characterized by HRMS and $^1\text{H NMR}$ using $\text{DMSO-}d_6$ as solvent, and purity of compounds was assessed via analytical rpHPLC (0% B to 100% B over 30 min gradient, Phenomenex C18 column, 300 Å, 4.6×250 mm, 214 nm λ). Compounds were repurified if found to be below 95%.

5-Isoxazolyl-Cha-Ile-amino-(3-(4-aminomethyl)piperidin-1-yl)propan-3-one (15). R_t 21.64 min; HRMS 569.3446 (calc), 569.3458 (found). $^1\text{H NMR}$ (400 MHz), δ 0.75–0.81 (m, 7H); 0.85–0.95 (m, 2H); 1.01–1.15 (m, 4H); 1.26–1.34 (m, 1H); 1.38–1.44 (m, 1H); 1.51–1.71 (m, 9H); 2.21 (t, 2H, $J = 7.41$ Hz); 2.57 (t, 1H, $J = 7.65$ Hz); 3.13–3.20 (m, 1H); 3.24–3.31 (m, 1H); 4.11 (dd, 1H, $J = 7.85, 16.44$ Hz); 4.52–4.57 (m, 1H); 7.00 (d, 1H, $J = 8.76$ Hz); 7.15–7.17 (m, 2H); 7.87–7.92 (m, 2H); 7.98 (t, 1H, $J = 5.70$ Hz); 8.75 (d, 1H, $J = 1.86$ Hz); 8.95 (d, 1H, $J = 8.32$ Hz).

5-Isoxazolyl-Cha-Ile-amino-[5-(4-aminomethyl)piperidin-1-yl]pentan-5-one (16). R_t 22.05 min; HRMS 597.3756 (calc), 597.3761 (found). $^1\text{H NMR}$ (400 MHz), δ 0.75–0.81 (m, 7H); 0.84–0.94 (m, 2H); 1.01–1.15 (m, 4H); 1.29–1.36 (m, 2H); 1.40–1.46 (m, 3H); 1.51–1.71 (m, 9H); 2.02 (t, 2H, $J = 7.31$ Hz); 2.63 (t, 1H, $J = 7.10$ Hz); 2.91–3.00 (m, 1H); 3.03–3.11 (m, 1H); 3.21 (dd, 1H, $J = 6.69, 14.43$ Hz); 4.10 (t, 3H, $J = 8.52$ Hz); 4.51–4.57 (m, 1H); 6.98 (d, 1H, $J = 8.29$ Hz); 7.13–7.17 (m, 3H); 7.82 (t, 1H, $J = 5.57$ Hz); 7.88 (d, 1H, $J = 8.98$ Hz); 7.93–7.99 (m, 1H); 8.75 (d, 1H, $J = 1.87$ Hz); 8.95 (d, 1H, $J = 8.28$ Hz).

Compounds 17 and 18. TCP resin (2×200 mg portions, 0.18 mmol scale) was first reacted with either Fmoc- β -Ala-OH (112 mg, 2 equiv) or Fmoc-5-aminovaleic acid (122 mg, 2 equiv) and DIPEA (62 μL , 2 equiv) dissolved in anhydrous DCM (2 mL) and then allowed to shake overnight. Compounds were then sequentially coupled with Fmoc-Ile-OH (2 equiv), Fmoc-Cha-OH (2 equiv), and isoxazole-5-carboxylic acid (2 equiv) in the presence of HOBt (4 equiv), DIC (2 equiv), and DIPEA (2 equiv) in 2 mL of DMF. Intermediates were then cleaved from resin using 5 mL of 20% TFA and 2.5% TIPS in DCM, solvent was removed under vacuum, and products were isolated via rpHPLC (25 mm OD, C18 column). Each was then dissolved in DMF (2 mL) and 3-(aminomethyl)pyridine (4 equiv), and BOP (2 equiv) was added and allowed to stir overnight. The solvent was removed in vacuo, and the crude products were purified by rpHPLC (Phenomenex C18 column, 300 Å, 22×250 mm, with a gradient of 0% B to 100% B over 30 min, solvent A 0.1% TFA in H_2O , solvent B 0.1% TFA, 10% acetonitrile, 90% H_2O). Compounds were characterized by HRMS and $^1\text{H NMR}$ using $\text{DMSO-}d_6$ as solvent, and purity of compounds was assessed via analytical rpHPLC (0% B to 100% B over 30 min gradient, Phenomenex C18 column, 300 Å, 4.6×250 mm, λ 214 nm). Compounds were repurified if found to be below 95%.

5-Isoxazolyl-Cha-Ile-amino-3-(pyridin-3-yl)methylamino]propan-3-one (17). R_t 21.29 min; HRMS 541.3133 (calc), 541.3153 (found). $^1\text{H NMR}$ (400 MHz), δ 0.75–0.79 (m, 8H); 0.84–0.86 (m, 2H); 1.00–1.15 (m, 4H); 1.25–1.32 (m, 1H); 1.38–1.44 (m, 1H); 1.50–1.70 (m, 9H); 2.33 (t, 2H, $J = 7.32$ Hz); 3.17–3.25 (m, 1H); 3.29–3.38 (m, 1H); 4.10 (t, 1H, $J = 8.68$ Hz); 4.34 (d, 1H, $J = 5.82$ Hz); 4.51–4.57 (m, 1H); 7.15 (d, 1H, $J = 1.91$ Hz); 7.62 (dd, 1H, $J = 5.27, 7.89$ Hz); 7.88 (d, 1H, $J = 8.87$ Hz); 7.97 (d, 1H, $J = 8.17$ Hz); 8.04 (t, 1H, $J = 11.17, 5.66$ Hz); 8.49 (t, 1H, $J = 11.90, 5.99$ Hz); 8.60 (s, 2H); 8.75 (d, 1H, $J = 1.90$ Hz); 8.96 (d, 1H, $J = 8.31$ Hz).

5-Isoxazolyl-Cha-Ile-amino-5-(pyridin-3-yl)methylamino]pentan-5-one (18). R_t 21.68 min; HRMS 569.3446 (calc), 569.3462 (found). $^1\text{H NMR}$ (400 MHz), δ 0.78–0.81 (m, 8H); 0.84–0.94 (m, 2H); 1.01–1.15 (m, 4H); 1.29–1.42 (m, 4H); 1.47–1.67 (m, 12H); 2.147

(t, 2H, $J = 7.39$ Hz); 2.92–3.00 (m, 1H); 3.05–3.13 (m, 1H); 4.10 (t, 1H, $J = 8.62$ Hz); 4.36 (d, 3H, $J = 5.85$ Hz); 4.51–4.57 (m, 1H); 7.15 (d, 1H, $J = 1.87$ Hz); 7.70 (dd, 1H, $J = 5.27, 7.93$ Hz); 7.88 (d, 1H, $J = 8.94$ Hz); 7.96 (t, 1H, $J = 11.18, 5.68$ Hz); 8.04 (d, 1H, $J = 11.44$ Hz); 8.45 (t, 1H, $J = 5.87$ Hz); 8.64 (s, 2H); 8.75 (d, 1H, $J = 1.89$ Hz); 8.95 (d, 1H, $J = 8.29$ Hz).

Compounds 19–28. TCP resin (3 g, substitution $0.9 \text{ mmol} \cdot \text{g}^{-1}$) was reacted with 4-(aminomethyl)piperidine (617 mg, 2 equiv) in anhydrous DCE (10 mL) and allowed to shake at rt overnight. Solution was removed, and resin was washed with DMF, treated with DTPM (1.14 g, 2 equiv) in DMF (12 mL), and then shaken for 2 h, after which the resin was washed with DMF and dried in vacuo. The resin was split into 10–300 mg portions, and each was reacted with either Fmoc-4-aminophenylacetic acid (202 mg), Fmoc-4-aminomethylbenzoic acid (202 mg), Fmoc-3-aminomethylbenzoic acid (202 mg), Fmoc-DL-pipecolic acid (190 mg), Fmoc-3-aminobenzoic acid (194 mg), Fmoc-4-aminobenzoic acid (194 mg), Fmoc- β -turn-dipeptide (Fmoc-Btd-OH, 237 mg), Fmoc-isonipecotic acid (190 mg), Fmoc-DL-nipecotic acid (190 mg), or Fmoc-Freidinger's lactam (236 mg) in a solution consisting of HOBt (4 equiv), DIC (2 equiv), and DIPEA (2 equiv) dissolved in DMF (2 mL). Solutions were left to shake overnight before the Fmoc protecting groups were removed by washing the resin twice with 1:1 piperidine/DMF for 3 min. Fmoc-Ile-OH (1.91 g, 10×2 equiv), HOBt (4 equiv), DIC (2 equiv), and DIPEA (2 equiv) were dissolved in DMF (20 mL), and 2 mL was added to each reaction. Fmoc-Cha-OH and isoxazole-5-carboxylic acid were then sequentially coupled following Fmoc SPPS. Compounds were cleaved from the resin by the addition of 20% TFA and 2.5% TIPS in DCM (5 mL) and stirred for 1 h. The solvent was removed under vacuum, and the crude products were purified by rpHPLC (Phenomenex C18 column, 300 Å, 22×250 mm, with a gradient of 0% B to 100% B over 30 min, solvent A 0.1% TFA in H_2O , solvent B 0.1% TFA, 10% acetonitrile, 90% H_2O). Compounds were characterized by HRMS and ^1H NMR using $\text{DMSO}-d_6$ as solvent, and purity of compounds was assessed via analytical rpHPLC (0% B to 100% B over 30 min gradient, Phenomenex C18 column, 300 Å, 4.6×250 mm, (λ 214 nm). Compounds were repurified if found to be below 95%.

5-Isoxazolyl-Cha-Ile-(3-[aminomethyl]phenyl)-(4-[aminomethyl]piperidin-1-yl)methanone (19). R_t 22.81 min; HRMS 609.3759 (calc), 609.3763 (found). ^1H NMR (400 MHz), δ 0.78–0.81 (m, 8H); 0.85–0.91 (m, 2H); 1.03–1.19 (m, 7H); 1.27–1.36 (m, 1H); 1.38–1.49 (m, 1H); 1.51–1.84 (m, 10H); 2.74 (t, 1H, $J = 6.07$ Hz); 4.19 (t, 1H, $J = 8.53$ Hz); 4.30 (dd, 1H, $J = 6.05, 9.03$ Hz); 4.53–4.59 (m, 1H); 7.16 (d, 1H, $J = 1.92$ Hz); 7.21–7.23 (m, 2H); 7.29 (d, 1H, $J = 7.87$ Hz); 7.36 (t, 1H, $J = 7.79$ Hz); 7.74 (s, 3H); 7.97 (d, 1H, $J = 11.95$ Hz); 8.54 (t, 1H, $J = 6.11$ Hz); 8.75 (d, 1H, $J = 1.89$ Hz); 8.95 (d, 1H, $J = 10.62$ Hz).

5-Isoxazolyl-Cha-Ile-(piperidin-3-yl)-(4-[aminomethyl]piperidin-1-yl)methanone (20). R_t 21.74 min; HRMS 587.3915 (calc), 587.3902 (found). ^1H NMR (400 MHz), δ 0.78–0.81 (m, 7H); 0.84–0.92 (m, 2H); 1.01–1.15 (m, 8H); 1.26–1.36 (m, 1H); 1.51–1.84 (m, 8H); 2.72 (t, 1H, $J = 5.87$ Hz); 4.20 (t, 1H, $J = 8.65$ Hz); 4.35 (dd, 1H, $J = 6.01, 8.88$ Hz); 4.54–4.60 (m, 1H); 8.14 (d, 1H, $J = 1.88$ Hz); 8.91 (d, 1H, $J = 9.94$ Hz).

5-Isoxazolyl-Cha-Ile-(4-aminophenyl)-(4-[aminomethyl]piperidin-1-yl)methanone (21). R_t 24.33 min; HRMS 595.3602 (calc), 595.3616 (found). ^1H NMR (400 MHz), δ 0.79–0.85 (m, 8H); 1.01–1.18 (m, 6H); 1.42–1.63 (m, 10H); 1.75–1.82 (m, 2H); 2.72 (d, 1H, $J = 8.27$ Hz); 4.27 (t, 1H, $J = 7.86$ Hz); 4.56–4.62 (m, 1H); 7.03 (d, 1H, $J = 8.02$ Hz); 7.12 (d, 1H, $J = 2.04$ Hz); 7.35 (t, 1H, $J = 8.22$ Hz); 7.54 (d, 1H, $J = 8.66$); 7.71 (s, 4H); 8.02 (d, 1H, $J = 9.02$ Hz); 8.84 (d, 1H, $J = 1.87$ Hz).

5-Isoxazolyl-Cha-Ile-4-aminophenyl-(4-[aminomethyl]piperidin-1-yl)ethan-2-one (22). R_t 22.87 min; HRMS 609.3759 (calc), 609.3782 (found). ^1H NMR (400 MHz), δ 0.81–0.87 (m, 9H); 1.06–1.21 (m, 4H); 1.24–1.34 (m, 1H); 1.48–1.80 (m, 12H); 2.65–2.71 (m, 1H); 2.92–3.00 (m, 1H); 3.64 (s, 1H); 4.30 (t, 1H, $J = 8.62$ Hz); 4.55–4.61 (m, 1H); 7.16 (dd, 1H, $J = 8.10, 9.97$ Hz); 7.50 (t, 1H,

$J = 7.71$ Hz); 7.69 (s, 2H); 8.04–8.11 (m, 2H); 8.75 (d, 1H, $J = 2.40$ Hz); 8.94 (d, 1H, $J = 8.18$ Hz).

5-Isoxazolyl-Cha-Ile-(4-[aminomethyl]phenyl)-(4-[aminomethyl]piperidin-1-yl)methanone (23). R_t 22.15 min; HRMS 609.3759 (calc), 609.3779 (found). ^1H NMR (400 MHz), δ 0.78–0.82 (m, 9H); 0.85–0.94 (m, 2H); 1.03–1.18 (m, 7H); 1.27–1.35 (m, 1H); 1.40–1.47 (m, 1H); 1.50–1.74 (m, 10H); 2.74 (t, 1H, $J = 6.31$ Hz); 4.19 (t, 1H, $J = 8.66$ Hz); 4.30 (dd, 1H, $J = 3.47, 6.73$ Hz); 4.54–4.60 (m, 1H); 7.15 (d, 1H, $J = 1.88$ Hz); 7.29–7.31 (m, 5H); 7.69 (s, 2H); 7.99 (d, 1H, $J = 12.27$ Hz); 8.55 (t, 1H, $J = 6.09$ Hz); 8.75 (d, 1H, $J = 1.85$ Hz); 8.96 (d, 1H, $J = 9.65$ Hz).

5-Isoxazolyl-Cha-Ile-(piperidin-4-yl)-(4-[aminomethyl]piperidin-1-yl)methanone (24). R_t 21.98 min; HRMS 587.3915 (calc), 587.3903 (found). ^1H NMR (400 MHz), δ 0.77–0.80 (m, 7H); 0.82–0.90 (m, 2H); 1.00–1.12 (m, 8H); 1.23–1.31 (m, 1H); 1.49–1.66 (m, 8H); 2.70 (t, 1H, $J = 5.87$ Hz); 4.07 (t, 1H, $J = 8.67$ Hz); 4.32 (dd, 1H, $J = 5.41, 7.42$ Hz); 4.54–4.60 (m, 1H); 7.137 (d, 1H, $J = 5.95$ Hz); 7.708 (s, 1H); 8.748 (d, 1H, $J = 10.69$ Hz).

5-Isoxazolyl-Cha-Ile-(3-aminophenyl)-(4-[aminomethyl]piperidin-1-yl)methanone (25). R_t 22.46 min; HRMS 595.3602 (calc), 595.3620 (found). ^1H NMR (400 MHz), δ 0.82–0.88 (m, 8H); 1.05–1.19 (m, 6H); 1.44–1.70 (m, 10H); 1.76–1.85 (m, 2H); 2.74 (d, 1H, $J = 7.04$ Hz); 4.30 (t, 1H, $J = 8.47$ Hz); 4.56–4.62 (m, 1H); 7.04 (d, 1H, $J = 7.59$ Hz); 7.16 (d, 1H, $J = 1.91$ Hz); 7.37 (t, 1H, $J = 7.97$ Hz); 7.57 (d, 1H, $J = 8.61$); 7.71 (s, 4H); 8.14 (d, 1H, $J = 8.73$ Hz); 8.75 (d, 1H, $J = 1.91$ Hz); 10.21 (s, 1H).

5-Isoxazolyl-Cha-Ile-(piperidin-2-yl)-(4-[aminomethyl]piperidin-1-yl)methanone (26). R_t 22.65 min (2 peaks for R- and S-enantiomers); HRMS 587.3915 (calc), 587.3929 (found). ^1H NMR (400 MHz), δ 0.78–0.82 (m, 7H); 0.84–0.92 (m, 2H); 1.01–1.15 (m, 8H); 1.26–1.36 (m, 1H); 1.51–1.84 (m, 8H); 2.72 (t, 1H, $J = 5.87$ Hz); 4.07 (t, 1H, $J = 8.67$ Hz); 4.32 (dd, 1H, $J = 6.38, 8.24$ Hz); 4.55–4.59 (m, 1H); 7.153 (t, 1H, $J = 1.76$ Hz); 8.755 (d, 1H, $J = 10.36$ Hz).

5-Isoxazolyl-Cha-Ile-(3R,6S)-6-amino-3-(4-[aminomethyl]piperidine-1-carbonyl)tetrahydro-2H-thiazolo(3,2-a)pyridin-5(3H)-one (27). R_t 22.05 min; HRMS 674.3694 (calc), 674.3680 (found).

5-Isoxazolyl-Cha-Ile-(R)-3-amino-1-([S]-1-[4-(aminomethyl)piperidin-1-yl]-4-methyl-1-oxopentan-2-yl)pyrrolidin-2-one (28). R_t 23.60 min; HRMS 672.4443 (calc), 672.4461 (found).

Compounds 30–36 (General Synthetic overview). Compounds were synthesized in solution phase using Boc-protected amino acids. For the initial coupling, the amino acid (1.2 equiv), HBTU (1.2 equiv), HOBT (3 equiv), and DIPEA (1.2 equiv) were dissolved in a volume of DMF. The solution was then added to an amino bearing C-terminal moiety and left to stir overnight at rt. The solutions were then diluted with ethyl acetate and washed twice with saturated NaHCO_3 . The organic phase was dried with MgSO_4 , and the solvent removed in vacuo. Boc protecting groups were removed from amino acids with a solution of 20% TFA in DCM stirred for 1 h. The solution was neutralized by washing with saturated NaHCO_3 (2 \times), dried with MgSO_4 , and then removed in vacuo. Subsequent amino acids and N-terminal carboxylic acids were then sequentially coupled under the same condition. Coupling was determined by ESI MS, with most reaching completion overnight. Crude products were purified by rpHPLC fitted with a tunable absorbance detector (λ 214 nm), using a Phenomenex C18 column (300 Å, 22×250 mm) with a gradient of 0% B to 100% B over 30 min (solvent A 0.1% TFA in H_2O , solvent B 0.1% TFA, 10% acetonitrile, 90% H_2O). Compounds were characterized by HRMS and ^1H NMR using $\text{DMSO}-d_6$ as solvent, and purity of compounds was assessed via analytical rpHPLC under varying conditions (0% B to 100% B over 30 min gradient, Phenomenex C18 column, 300 Å, 4.6×250 mm, (λ 214 nm). Compounds were repurified by further gradient-varied rpHPLC if necessary until >95% pure, as assessed by analytical HPLC.

5-Isoxazolyl-Cha-Ile-4-aminophenyl-(4morpholin-1-yl)ethan-2-one (30). TCP resin (200 mg, substitution $0.9 \text{ mmol} \cdot \text{g}^{-1}$) was first reacted with Fmoc-4-aminophenylacetic acid (269 mg, 4 equiv)

in the presence of DIPEA (124 μ L, 4 equiv) in DMF (2 mL) and allowed to shake overnight. The Fmoc protecting group was removed with 2×3 min washes with excess 1:1 piperidine/DMF, and the resin was washed with DMF. Fmoc-Ile-OH (127 mg, 2 equiv), Fmoc-Cha-OH (142 mg, 2 equiv), and isoxazole-5-carboxylic acid (41 mg, 2 equiv) were then sequentially coupled following standard Fmoc-SPPS, using HOBT (49 mg, 4 equiv), DIC (56 μ L, 2 equiv), and DIPEA (62 μ L, 2 equiv) in DMF (2 mL). The intermediate was cleaved from resin in a solution of 20% TFA and 2.5% TIPS in DCM (5 mL) stirred for 1.5 h and then filtered in a sintered glass funnel. The filtrate was removed under vacuum, and the product was isolated via rpHPLC (25 mm OD, C18 column). HOBT (2 equiv), DIC (2 equiv), and DIPEA (2 equiv) were added to the intermediate (30 mg) and dissolved in DMF (2 mL), followed by the addition of morpholine (14 μ L, 4 equiv), and the solution was left to stir overnight at rt. Ethyl acetate (20 mL) was added to the solution, it was washed with 3×20 mL aliquots of saturated NaHCO_3 , and the organic phases were combined, dried with MgSO_4 , and evaporated in vacuo. The crude product was isolated via rpHPLC fitted with a tunable absorbance detector (λ 214 nm), using a Phenomenex C18 column (300 \AA , 22×250 mm) with a gradient of 0% B to 100% B over 30 min (solvent A 0.1% TFA in H_2O , solvent B 0.1% TFA, 10% acetonitrile, 90% H_2O) to yield **30** as a white solid (8.7 mg, 0.015 mmol, 8% yield). R_t 21.89 min; HRMS [MH^+] 582.3286 (calc), 582.3298 (found). ^1H NMR (400 MHz), δ 0.81–0.88 (m, 8H); 1.06–1.16 (m, 4H); 1.46–1.67 (m, 10H); 1.74–1.83 (m, 2H); 2.65–2.71 (m, 1H); 2.92–3.00 (m, 1H); 3.64 (s, 1H); 4.30 (t, 1H, $J = 8.69$ Hz); 4.47 (t, 1H, $J = 8.42$ Hz); 7.74 (d, 1H, $J = 6.00$ Hz); 8.11 (d, 1H, 5.76 Hz); 8.19 (d, 1H, $J = 8.72$ Hz); 10.06 (s, 1H).

5-Isoxazolyl-Cha-Ile-3,4-dihydroisoquinoline (31). $R_t = 31.79$ min; HRMS [MH^+] 495.2966 (calc), 495.2984 (found). ^1H NMR (400 MHz), δ 0.77–0.84 (m, 7H); 1.02–1.13 (m, 4H); 1.30–1.36 (m, 1H); 1.46–1.65 (m, 7H); 1.77–1.85 (m, 1H); 2.74 (t, 1H, $J = 5.91$ Hz); 2.80–2.91 (m, 1H); 3.56–3.63 (m, 1H); 3.71–3.80 (m, 1H); 3.86–3.92 (m, 1H); 4.47–4.57 (m, 2H); 4.63–4.73 (m, 2H); 7.14–7.17 (m, 4H); 8.21 (t, 1H, $J = 8.45$ Hz); 8.74 (d, 1H, $J = 1.88$ Hz); 8.86–8.90 (m, 1H).

5-Isoxazolyl-Cha-Ile-1-amino-naphthalene (32). $R_t = 23.27$ min; HRMS [MH^+] 505.2809 (calc), 505.2821 (found). ^1H NMR (400 MHz), δ 0.90 (t, 2H, $J = 7.37$ Hz); 1.00 (d, 2H, $J = 6.75$ Hz); 1.20–1.25 (m, 2H); 1.53–1.64 (m, 4H); 1.70–1.73 (m, 2H); 4.51 (t, 1H, $J = 8.70$ Hz); 4.60–4.66 (m, 2H); 7.17 (d, 1H, $J = 1.90$ Hz); 7.47–7.54 (m, 2H); 7.60 (d, 1H, $J = 7.34$ Hz); 7.78 (t, 1H, $J = 8.19$ Hz); 7.94 (d, 1H, $J = 9.43$ Hz); 8.02 (d, 1H, $J = 6.73$ Hz); 8.23 (d, 1H, $J = 8.21$ Hz); 8.75 (d, 1H, $J = 1.86$ Hz); 9.00 (d, 1H, $J = 8.33$ Hz).

5-Isoxazolyl-Cha-Ile-(4-phenyl)piperazine (33). $R_t = 28.61$ min; HRMS [MH^+] 424.3231 (calc), 524.3243 (found). ^1H NMR (400 MHz), δ 0.78–0.72 (m, 6H); 0.84–0.89 (m, 2H); 1.02–1.11 (m, 4H); 1.22–1.30 (m, 1H); 1.45–1.64 (m, 8H); 1.77–1.83 (m, 1H); 2.94–3.13 (m, 5H); 3.49–3.77 (m, 8H); 4.49–4.55 (m, 1H); 4.59 (t, 1H, $J = 8.64$ Hz); 6.79 (t, 1H, $J = 7.27$ Hz); 6.92 (d, 2H, $J = 8.84$); 7.10 (d, 1H, $J = 4.00$ Hz); 7.20 (dd, 1H, $J = 7.28, 8.74$ Hz); 8.19 (d, 1H, $J = 8.75$ Hz); 8.88 (d, 1H, $J = 8.26$ Hz).

5-Isoxazolyl-Cha-Ile-4-(o-tolyl)piperazine (34). $R_t = 32.85$ min; HRMS [MH^+] 538.3388 (calc), 538.3399 (found). ^1H NMR (400 MHz), δ 0.81–0.85 (m, 6H); 0.87–0.95 (m, 2H); 1.04–1.12 (m, 4H); 1.28–1.36 (m, 1H); 1.47–1.53 (m, 1H); 1.55–1.70 (m, 7H); 1.80–1.86 (m, 1H); 2.26 (s, 2H); 2.65–2.70 (m, 1H); 2.75–2.83 (m, 4H); 3.48–3.53 (m, 1H); 3.62–3.68 (m, 1H); 3.72–3.78 (m, 2H); 6.94–6.99 (m, 2H); 7.14 (d, 1H, $J = 1.91$); 8.22 (d, 1H, $J = 8.83$ Hz); 8.74 (d, 1H, $J = 1.90$ Hz); 8.93 (d, 1H, $J = 8.29$ Hz).

5-Isoxazolyl-Cha-Ile-1-aminobiphenyl (35). $R_t = 33.45$ min; HRMS [MH^+] 531.2966 (calc), 531.2977 (found). ^1H NMR (400 MHz), δ 0.77–0.93 (m, 2H); 1.07–1.18 (m, 3H); 1.24–1.33 (m, 1H); 1.46–1.52 (m, 1H); 1.56–1.68 (m, 7H); 4.51–4.57 (m,

2H); 7.15 (d, 1H, $J = 2.95$); 7.26–7.38 (m, 8H); 7.51 (d, 1H, $J = 8.52$ Hz); 8.75 (d, 1H, $J = 1.91$ Hz); 8.95 (d, 1H, $J = 8.12$ Hz); 9.35 (s, 1H).

5-Isoxazolyl-Cha-Ile-spiroindane-1,4'-piperidine (36). $R_t = 35.00$ min; HRMS [MH^+] 549.3435 (calc), 549.3451 (found). ^1H NMR (400 MHz), δ 0.79–0.82 (m, 6H); 1.03–1.14 (m, 4H); 1.42–1.60 (m, 10H); 2.02–2.08 (m, 2H); 2.87 (t, 1H, $J = 7.40$ Hz); 4.05 (t, 2H, $J = 10.46$ Hz); 4.35 (d, 2H, $J = 13.49$ Hz); 4.54–4.66 (m, 2H); 7.03 (d, 1H, $J = 6.53$ Hz); 7.12 (d, 1H, $J = 5.10$ Hz); 7.14–7.16 (m, 4H); 7.20 (d, 1H, $J = 5.42$ Hz); 8.12 (d, 1H, $J = 9.74$ Hz); 8.27 (d, 1H, $J = 9.64$ Hz); 8.75 (d, 1H, $J = 1.89$ Hz); 8.95 (d, 1H, $J = 8.38$ Hz).

Intracellular Calcium Efflux Assay and Dye buffer. To Hank's balanced salt solution (HBSS, 1 L) diluted 1 in 10 (1 \times) with distilled water was added 1 M HEPES (20 mL) and probenecid (710 mg) dissolved in 1 N NaOH (5 mL); pH was then adjusted to 7.4. Aliquots of the fluorescent calcium indicator Fluo-3 a.m. (2 mM) dissolved in DMSO (25 μ L), FCS (120 μ L), and Pluronic acid (F-127, 25 μ L) were dissolved in assay buffer (12 mL) prior to use.

Sample Preparation. Stock solutions of agonists were prepared by weighing compounds in Eppendorf vials and dissolving them in a volume of DMSO to give a final concentration of 10 mM. Two more stock solutions were prepared by serially diluting the 10 mM sample with DMSO to give 500 and 10 μ M. These solutions were then diluted to 4 mL by dissolving 80 μ L of the 10 mM, 500 μ M, and 10 μ M standards in 3.92 mL of assay buffer to give three working solutions of 200, 10, and 0.2 μ M. Similarly, blanks were prepared by diluting DMSO (80 μ L) to 4 mL with assay buffer. Using two pumps during the assay to alter the volume of working stock to volume of blank delivered (so that the final volume is always 100 μ L), final concentrations in the range of 10 nM to 100 μ M are achieved and the concentration of DMSO is consistently 2%.

Assay Protocol. To adhere intact human embryonic kidney cells (HEK293) or colon carcinoma cells (HT29) to the base of a 96-well clear-bottomed black-walled assay plate (Corning), they were incubated at 37 $^\circ\text{C}$ overnight in either Dulbecco's modified essential serum (Gibco) or RPMI 1640 medium, supplemented with 2 mM L-glutamine (Gibco), 10% FCS, 0.1 mM MEM nonessential amino acids (Invitrogen), penicillin (100 U/mL), and streptomycin (100 U/mL). At 1 h before assaying, the medium was removed and cells were incubated with 100 μ L per well of dye loading buffer; this was removed prior to the assay, and wells were washed two times with assay buffer before a final volume of assay buffer (100 μ L) was added to each well. Fluorescence was measured (excitation 495 nm, emission 520 nm) from the bottom of the plate for 60 s using a Polarstar (BMG LABTECH) fluorescent plate reader, with blank delivered at 10 s and agonist delivered after 12 s to a final volume of 100 μ L.⁶³ For dose dependent concentration curves, agonists were delivered to cells with final concentrations of 0.01, 0.03, 0.1, 0.3, 1, 3, 10, 30, and 100 μ M, using three replicates per concentration. Ca^{2+} efflux is reported as percent response of the Ca^{2+} ionophore A-23187 (calcimycin) and plotted as mean \pm SEM.

Statistical Analysis. For agonist and antagonist assays, non-linear regression was performed using Prism 5 (GraphPad Software, San Diego, CA).

Serum Stability Assay. A stock solution of compound 19 (20 mM) was prepared in water with 2% DMSO. An aliquot (500 μ L) was then added to filtered FCS (4.5 mL) at 37 $^\circ\text{C}$. At intervals of 0, 5, 15, 30, 60, 120, 180, and 240 min, 500 μ L was removed and added to 1.5 mL of MeCN and then centrifuged at 2500 rpm for 5 min. A total of 1 mL of the supernatant was removed and analyzed via LCMS (20% B to 100% B in 20 min). Data were plotted as a percentage of the peak area calculated from $t = 0$ s samples.

Acknowledgment. We thank the Australian Research Council (ARC) for a Federation Fellowship to D.P.F. and

both ARC (Grants FF668733 and DP1093245) and the National Health and Medical Research Council of Australia (Grants 569595 and APP1000745) for research support.

Supporting Information Available: Schemes S1–4 for synthesis of **14** and **15** (Scheme S1), **16–19** (Scheme S2), **20** and **21** (Scheme S3), and **22** (Scheme S4) and analytical rp-HPLC traces for agonist **19** (GB110) and antagonist **36** (GB83). This material is available free of charge via the Internet at <http://pubs.acs.org>.

References

- Blakeney, J. S.; Reid, R. C.; Le, G. T.; Fairlie, D. P. Nonpeptidic Ligands For Peptide-Activated GPCRs. *Chem. Rev.* **2007**, *107*, 2960–3041.
- Harmar, A. J.; Hills, R. A.; Rosser, E. M.; Jones, M.; Buneman, O. P.; Dunbar, D. R.; Greenhill, S. D.; Hale, V. A.; Sharman, J. L.; Bonner, T. I.; Catterall, W. A.; Davenport, A. P.; Delagrèze, P.; Dollery, C. T.; Foord, S. M.; Gutman, G. A.; Laudet, V.; Neubig, R. R.; Ohlstein, E. H.; Olsen, R. W.; Peters, J.; Pin, J. P.; Ruffolo, R. R.; Searls, D. B.; Wright, M. W.; Spedding, M. IUPHAR-DB: The IUPHAR Database of G Protein-Coupled Receptors and Ion Channels. *Nucleic Acids Res.* **2009**, *37* (Database issue), D680–D685.
- Barry, G. D.; Le, G. T.; Fairlie, D. P. Agonists and Antagonists of Protease Activated Receptors (PARs). *Curr. Med. Chem.* **2006**, *13*, 243–265.
- Cottrell, G. S.; Amadesi, S.; Schmidlin, F.; Bunnett, N. Protease-activated receptor 2: activation, signalling and function. *Biochem. Soc. Trans.* **2003**, *31*, 1191–1197.
- Steinhoff, M.; Buddenkotte, J.; Shpacovitch, V.; Rattenholl, A.; Moormann, C.; Vergnolle, N.; Luger, T. A.; Hollenberg, M. D. Proteinase-Activated Receptors: Transducers of Proteinase-Mediated Signaling in Inflammation and Immune Response. *Endocr. Rev.* **2005**, *26*, 1–43.
- MacFarlane, S. R.; Scatter, M. J.; Kanke, T.; Hunter, G. D.; Plevin, R. Proteinase-Activated Receptors. *Pharmacol. Rev.* **2001**, *53*, 245–282.
- Ossovskaya, V. S.; Bunnett, N. W. Protease-Activated Receptors: Contribution to Physiology and Disease. *Physiol. Rev.* **2003**, *84*, 579–621.
- Berger, P.; Tunon-De-Lara, J. M.; Savineau, J.-P.; Marthan, R. Signal Transduction in Smooth Muscle Selected Contribution: Tryptase-Induced PAR-2-Mediated Ca²⁺ Signaling in Human Airway Smooth Muscle Cells. *J. Appl. Physiol.* **2001**, *91*, 995–1003.
- Fyfe, M.; Bergstrom, M.; Aspengren, S.; Peterson, A. PAR-2 Activation in Intestinal Epithelial Cells Potentiates Interleukin-1 β -Induced Chemokine Secretion via MAP Kinase Signaling Pathways. *Cytokine* **2005**, *31*, 358–367.
- Myatt, A.; Hill, S. J. Trypsin Stimulates the Phosphorylation of p42.44 Mitogen-Activated Protein Kinases via the Proteinase-Activated Receptor-2 and Protein Kinase C Epsilon in Human Cultured Prostate Stromal Cells. *Prostate* **2005**, *64*, 175–185.
- Darmoul, D.; Gratio, V.; Devaud, H.; Laburthe, M. Protease-Activated Receptor 2 in Colon Cancer: Trypsin-Induced MAPK Phosphorylation and Cell Proliferation Are Mediated by Epidermal Growth Factor Receptor Transactivation. *J. Biol. Chem.* **2004**, *279*, 20927–20934.
- Scott, G.; Leopardi, S.; Parker, L.; Babiarz, L.; Seiberg, M.; Han, R. The Proteinase-Activated Receptor-2 Mediates Phagocytosis in a Rho-Dependent Manner in Human Keratinocytes. *J. Invest. Dermatol.* **2003**, *121*, 529–541.
- Miyata, S.; Koshikawa, N.; Yasumitsu, H.; Miyazaki, K. Trypsin Stimulates Integrin $\alpha(5)\beta(1)$ -Dependent Adhesion to Fibronectin and Proliferation of Human Gastric Carcinoma Cells through Activation of Proteinase-Activated Receptor-2. *J. Biol. Chem.* **2000**, *275*, 4592–4598.
- Darmoul, D.; Marie, J. C.; Devaud, H.; Gratio, V.; Laburthe, M. Initiation of Human Colon Cancer Cell Proliferation by Trypsin Acting at Protease-Activated Receptor-2. *Br. J. Cancer* **2001**, *85*, 772–779.
- Shimamoto, R.; Sawada, T.; Uchima, Y.; Inoue, M.; Kimura, K.; Yamashita, Y.; Yamada, N.; Nishihara, T.; Ohira, M.; Hirakawa, K. A Role for Protease-Activated Receptor-2 in Pancreatic Cancer Cell Proliferation. *Int. J. Oncol.* **2004**, *24*, 1401–1406.
- Masamune, A.; Kikuta, K.; Satoh, M.; Suzuki, N.; Shimosegawa, T. Protease-Activated Receptor-2 Mediated Proliferation and Collagen Production of Rat Pancreatic Stellate Cells. *J. Pharmacol. Exp. Ther.* **2005**, *312*, 651–658.
- Wilson, S.; Greer, B.; Hooper, J.; Zijlstra, A.; Walker, B.; Quigley, J.; Hawthorne, S. The Membrane-Anchored Serine Protease, TMPRSS2, Activates PAR-2 in Prostate Cancer Cells. *Biochem. J.* **2005**, *388*, 967–972.
- Ferrell, W. R.; Lockhart, J. C.; Kelso, E. B.; Dunning, L.; Plevin, R.; Meek, S. E.; Smith, A. J. H.; Hunter, G. D.; McLean, J. S.; McGarry, F.; Ramage, R.; Jiang, L.; Kanke, T.; Kawagoe, J. Essential Role for Proteinase-Activated Receptor-2 in Arthritis. *J. Clin. Invest.* **2003**, *111*, 35–41.
- Cenac, N.; Garcia-Villar, R.; Ferrier, L.; Larauche, M.; Vergnolle, N.; Bunnett, N. W.; Coelho, A. M.; Fioramonti, J.; Bueno, L. Proteinase-Activated Receptor-2-Induced Colonic Inflammation in Mice: Possible Involvement of Afferent Neurons, Nitric Oxide, and Paracellular Permeability. *J. Immunol.* **2003**, *170*, 4296–4300.
- Cenac, N.; Chin, A. C.; Garcia-Villar, R.; Salvador-Cartier, C.; Ferrier, L.; Vergnolle, N.; Buret, A. G.; Fioramonti, J.; Bueno, L. PAR2 Activation Alters Colonic Paracellular Permeability in Mice via IFN- γ -Dependent and -Independent Pathways. *J. Physiol.* **2004**, *558*, 913–925.
- Kawabata, A.; Kuroda, R.; Kuroki, N.; Nishikawa, H.; Kawai, K. Dual Modulation by Thrombin of the Motility of Rat Oesophageal Muscularis Mucosae via Two Distinct Protease-Activated Receptors (PARs): a Novel Role for PAR-4 As Opposed to PAR-1. *Br. J. Pharmacol.* **2000**, *131*, 578–584.
- Holzhausen, M.; Spolidorio, L.; Vergnolle, N. Role of Protease-Activated Receptor-2 in Inflammation, and Its Possible Implications As a Putative Mediator of Periodontitis. *Mem. Inst. Oswaldo Cruz* **2005**, *100*, 177–180.
- Buddenkotte, J.; Strohs, C.; Engels, I. H.; Moormann, C.; Shpacovitch, V. M.; Seeliger, S.; Vergnolle, N.; Vestweber, D.; Luger, T. A.; Schulze-Osthoff, K.; Steinhoff, M. Agonists of Proteinase-Activated Receptor-2 Stimulate Upregulation of Intercellular Cell Adhesion Molecule-1 in primary Human Keratinocytes via Activation of NH-kappa B. *J. Invest. Dermatol.* **2005**, *124*, 38–45.
- Hansen, K. K.; Sherman, P. M.; Cellars, L.; Andrade-Gordon, P.; Pan, Z.; Baruch, A.; Wallace, J. L.; Hollenberg, M. D.; Vergnolle, N. A Major Role for Proteolytic Activity and Proteinase-Activated Receptor-2 in the Pathogenesis of Infectious Colitis. *Proc. Natl. Acad. Sci. U.S.A.* **2005**, *102*, 8363–8368.
- Lee, Y. C. G.; Knight, D. A.; Lane, K. B.; Cheng, D. S.; Koay, M. A.; Teixeira, L. R.; Nesbitt, J. C.; Chambers, R. C.; Thompson, P. J.; Light, R. W. Activation of Proteinase-Activated Receptor-2 in Mesothelial Cells Induces Pleural Inflammation. *Am. J. Physiol. Lung Cell. Mol. Physiol.* **2005**, *288*, 734–740.
- Maeda, K.; Hirota, M.; Kimura, Y.; Ichihara, A.; Ohmuraya, M.; Sugita, H.; Ogawa, M. Proinflammatory Role of Trypsin and Protease-activated Receptor-2 in a Rat Model of Acute Pancreatitis. *Pancreas* **2005**, *31*, 54–62.
- Reed, C. E.; Kita, H. The Role of Protease Activation of Inflammation in Allergic Respiratory Diseases. *J. Allergy Clin. Immunol.* **2004**, *114*, 997–1008.
- Cicala, C. Protease Activated Receptor 2 and the Cardiovascular System. *Br. J. Pharmacol.* **2002**, *135*, 14–20.
- Kawabata, A.; Kinoshita, M.; Nishikawa, H.; Kuroda, R.; Nishida, M.; Araki, H.; Arizono, N.; Oda, Y.; Kakehi, K. The Protease-Activated Receptor-2 Agonist Induces Gastric Mucus Secretion and Mucosal Cytoprotection. *J. Clin. Invest.* **2001**, *107*, 1443–1450.
- Fiorucci, S.; Mencarelli, A.; Palazzetti, B.; Distrutti, E.; Vergnolle, N.; Hollenberg, M. D.; Wallace, J. L.; Morelli, A.; Cirino, G. Proteinase-Activated Receptor 2 Is an Anti-Inflammatory Signal for Colonic Lamina Propria Lymphocytes in a Mouse Model of Colitis. *Proc. Natl. Acad. Sci. U.S.A.* **2001**, *98*, 13936–13941.
- Cocks, T. M.; Moffatt, J. D. Protease-Activated Receptors: Sentries for Inflammation? *Trends Pharmacol. Sci.* **2000**, *21*, 103–108.
- Cocks, T. M.; Moffatt, J. D. Protease-Activated Receptor-2 (PAR2) in the Airways. *Pulm. Pharmacol. Ther.* **2001**, *14*, 183–191.
- Schmidlin, F.; Amadesi, S.; Vidali, R.; Trevisani, M.; Martinet, N.; Caughey, G.; Tognetto, M.; Cavallero, G.; Mapp, C.; Geppetti, P.; Bunnett, N. W. Expression and Function of Proteinase-Activated Receptor 2 in Human Bronchial Smooth Muscle. *Am. J. Respir. Crit. Care Med.* **2001**, *164*, 1276–1281.
- Fiorucci, S.; Antonelli, E.; Distrutti, E.; Severino, B.; Fiorentina, R.; Baldoni, M.; Caliendo, G.; Santagada, V.; Morelli, A.; Cirino, G. PAR1 Antagonism Protects against Experimental Liver Fibrosis. Role of Proteinase Receptors in Stellate Cell Activation. *Hepatology* **2004**, *39*, 365–375.
- Gaca, M. D. A.; Zhou, X.; Benyon, R. C. Regulation of Hepatic Stellate Cell Proliferation and Collagen Synthesis by Proteinase-Activated Receptors. *J. Hepatol.* **2002**, *36*, 362–369.
- Campo, B. A. D.; Henry, P. J. Stimulation of Protease-Activated Receptor-2 Inhibits Airway Eosinophilia, Hyperresponsiveness

- and Bronchoconstriction in a Murine Model of Allergic Inflammation. *Br. J. Pharmacol.* **2005**, *144*, 1100–1108.
- (37) Su, X.; Camerer, E.; Hamilton, J. R.; Coughlin, S. R.; Matthey, M. A. Protease-Activated Receptor-2 Activation Induces Acute Lung Inflammation by Neuropeptide-Dependent Mechanisms. *J. Immunol.* **2005**, *175*, 2598–2605.
- (38) Versteeg, H. H.; Schaffner, F.; Kerver, M.; Petersen, H. H.; Ahamed, J.; Felding-Habermann, B.; Takada, Y.; Mueller, B. M.; Ruf, W. Inhibition of Tissue Factor Signaling Suppresses Tumor Growth. *Blood* **2008**, *111*, 190–199.
- (39) Uusitalo-Jarvinen, H.; Kurokawa, T.; Mueller, B. M.; Andrade-Gordon, P.; Friedlander, M.; Ruf, W. Role of Protease Activated Receptor 1 and 2 Signaling in Hypoxia-Induced Angiogenesis. *Arterioscler., Thromb., Vasc. Biol.* **2007**, *27*, 1456–1462.
- (40) Ramelli, G.; Fuertes, S.; Narayan, S.; Busso, N.; Acha-Orbea, H.; So, A. Protease-Activated Receptor 2 Signalling Promotes Dendritic Cell Antigen Transport and T-Cell Activation in Vivo. *Immunology* **2010**, *129*, 20–27.
- (41) Redecha, P.; Franzke, C. W.; Ruf, W.; Mackman, N.; Girardi, G. Neutrophil Activation by the Tissue Factor/Factor VIIa/ PAR2 Axis Mediates Fetal Death in a Mouse Model of Antiphospholipid Syndrome. *J. Clin. Invest.* **2008**, *118*, 3453–3461.
- (42) Shichijo, M.; Kondo, S.; Ishimori, M.; Watanabe, S.; Helin, H.; Yamasaki, T.; Stevens, M. E.; Gantner, F.; Bacon, K. B. PAR-2 Deficient CD4+ T Cells Exhibit Downregulation of IL-4 and Upregulation of IFN- γ after Antigen Challenge in Mice. *Allergol. Int.* **2006**, *55*, 271–278.
- (43) Takizawa, T.; Tamiya, M.; Hara, T.; Matsumoto, J.; Saito, N.; Kanke, T.; Kawagoe, J.; Hattori, Y. Abrogation of Bronchial Eosinophilic Inflammation and Attenuated Eotaxin Content in Protease-Activated Receptor 2-Deficient Mice. *J. Pharmacol. Sci.* **2005**, *98*, 99–102.
- (44) Lindner, J. R.; Kahn, M. L.; Coughlin, S. R.; Sambrano, G. R.; Schauble, E.; Bernstein, D.; Foy, D.; Hafezi-Moghadam, A.; Ley, K. Delayed Onset of Inflammation in Protease-Activated Receptor-2-Deficient Mice. *J. Immunol.* **2000**, *165*, 6504–6510.
- (45) Ishikawa, C.; Tsuda, T.; Konishi, H.; Nakagawa, N.; Yamanishi, K. Tetracyclines Modulate Protease-Activated Receptor 2-Mediated Proinflammatory Reactions in Epidermal Keratinocytes. *Antimicrob. Agents Chemother.* **2009**, *53*, 1760–1765.
- (46) Rohani, M. G.; Beyer, R. P.; Hacker, B. M.; Dommisch, H.; Dale, B. A.; Chung, W. O. Modulation of Expression of Innate Immunity Markers CXCL5/ENA-78 and CCL20/MIP3 α by Protease-Activated Receptors (PARs) in Human Gingival Epithelial Cells. *Innate Immun.* **2010**, *16*, 104–114.
- (47) Kawabata, A.; Matsunami, M.; Tsutsumi, M.; Ishiki, T.; Fukushima, O.; Sekiguchi, F.; Kawao, N.; Minami, T.; Kanke, T.; Saito, N. Suppression of Pancreatitis-Related Allodynia/Hyperalgesia by Proteinase-Activated Receptor-2 in Mice. *Br. J. Pharmacol.* **2006**, *148*, 54–60.
- (48) Afkhami-Goli, A.; Noorbakhsh, F.; Keller, A. J.; Vergnolle, N.; Westaway, D.; Jhamandas, J. H.; Andrade-Gordon, P.; Hollenberg, M. D.; Arab, H.; Dyck, R. H.; Power, C. Proteinase-Activated Receptor-2 Exerts Protective and Pathogenic Cell Type-Specific Effects in Alzheimer's Disease. *J. Immunol.* **2007**, *179*, 5493–5503.
- (49) Versteeg, H. H.; Schaffner, F.; Kerver, M.; Ellies, L. G.; Andrade-Gordon, P.; Mueller, B. M.; Ruf, W. Protease-Activated Receptor (PAR) 2, but not PAR1, Signaling Promotes the Development of Mammary Adenocarcinoma in Polyoma Middle T Mice. *Cancer Res.* **2008**, *68*, 7219–7227.
- (50) Vergnolle, N. Proteinase-Activated Receptors and Nociceptive Pathways. *Drug Dev. Res.* **2003**, *59*, 382–385.
- (51) Grand, R. J.; Turnell, A. S.; Grabham, P. W. Cellular Consequences of Thrombin-Receptor Activation. *Biochem. J.* **1996**, *313* (Pt 2), 353–368.
- (52) Vergnolle, N.; Bunnett, N. W.; Sharkey, K. A.; Brussee, V.; Compton, S. J.; Grady, E. F.; Cirino, G.; Gerard, N.; Basbaum, A. I.; Andrade-Gordon, P.; Hollenberg, M. D.; Wallace, J. L. Proteinase-Activated Receptor-2 and Hyperalgesia: A Novel Pain Pathway. *Nat. Med.* **2001**, *7*, 821–826.
- (53) Abey, H. T.; Fairlie, D. P.; Moffatt, J. D.; Balzary, R. W.; Cocks, T. M. Protease-Activated Receptor-2 Peptides Activate Neurokinin-1 Receptors in the Mouse Isolated Trachea. *J. Pharmacol. Exp. Ther.* **2006**, *317*, 598–605.
- (54) Kelso, E. B.; Lockhart, J. C.; Hembrough, T.; Dunning, L.; Plevin, R.; Hollenberg, M. D.; Sommerhoff, C. P.; McLean, J. S.; Ferrell, W. R. Therapeutic Promise of Proteinase Activated Receptor-2 Antagonism in Joint Inflammation. *J. Pharmacol. Exp. Ther.* **2006**, *316*, 1017–1024.
- (55) Kanke, T.; Kabeya, M.; Kubo, S.; Kondo, S.; Yasuoka, K.; Tagashira, J.; Ishiwata, H.; Saka, M.; Furuyama, T.; Nishiyama, T.; Doi, T.; Hattori, Y.; Kawabata, A.; Cunningham, M. R.; Plevin, R. Novel Antagonists for Proteinase-Activated Receptor 2: Inhibition of Cellular and Vascular Responses in Vitro and in Vivo. *Br. J. Pharmacol.* **2009**, *158*, 361–371.
- (56) Al-Ani, B.; Saifeddine, M.; Kawabata, A.; Hollenberg, M. D. Proteinase Activated Receptor 2: Role of Extracellular Loop 2 for Ligand-Mediated Activation. *Br. J. Pharmacol.* **1999**, *128*, 1105–1113.
- (57) Blackhart, B. D.; Emilsson, K.; Nguyen, D.; Teng, W.; Martelli, A. J.; Nystedt, S.; Sundelin, J.; Scarborough, R. M. Ligand Cross-Reactivity within the Protease-Activated Receptor Family. *J. Biol. Chem.* **1996**, *271*, 16466–16471.
- (58) Hollenberg, M. D.; Saifeddine, M.; al-Ani, B. Proteinase-Activated Receptor-2 in Rat Aorta: Structural Requirements for Agonist Activity of Receptor-Activating Peptides. *Mol. Pharmacol.* **1996**, *49*, 229–233.
- (59) Maryanoff, B. E.; Santulli, R. J.; McComsey, D. F.; Hoekstra, W. J.; Hoey, K.; Smith, C. E.; Addo, M.; Darrow, A. L.; Andrade-Gordon, P. Proteinase-Activated Receptor-2 (PAR-2): Structure-Function Study of Receptor Activation by Diverse Peptides Related to Tethered-Ligand Epitopes. *Arch. Biochem. Biophys.* **2001**, *386*, 195–204.
- (60) Kawabata, A.; Kanke, T.; Yonezawa, D.; Ishiki, T.; Saka, M.; Kabeya, M.; Sekiguchi, F.; Kubo, S.; Kuroda, R.; Iwaki, M.; Katsura, K.; Plevin, R. Potent and Metabolically Stable Agonists for Protease-Activated Receptor-2: Evaluation of Activity in Multiple Assay Systems in Vitro and in Vivo. *J. Pharmacol. Exp. Ther.* **2004**, *309*, 1098–1107.
- (61) McGuire, J. J.; Saifeddine, M.; Triggle, C. R.; Sun, K.; Hollenberg, M. D. 2-Furoyl-LIGRLO-amide: A Potent and Selective Proteinase-Activated Receptor 2 Agonist. *J. Pharmacol. Exp. Ther.* **2004**, *309*, 1124–1131.
- (62) Kanke, T.; Ishiwata, H.; Kabeya, M.; Saka, M.; Doli, T.; Hattori, Y.; Kawabata, A.; Plevin, R. Binding of a Highly Potent Protease-Activated Receptor-2 (PAR2) Activating Peptide, [³H]2-furoyl-LIGRLO-NH₂, to Human PAR2. *Br. J. Pharmacol.* **2005**, *145*, 255–263.
- (63) Devlin, M. G.; Pfeiffer, B.; Flanagan, B.; Beyer, R. L.; Cocks, T. M.; Fairlie, D. P. Hepta and Octa Peptide Agonists of Protease-Activated Receptor 2. *J. Pept. Sci.* **2007**, *13*, 856–861.
- (64) Barry, G. D.; Suen, J. Y.; Low, H. B.; Pfeiffer, B.; Flanagan, B.; Halili, M.; Le, G. T.; Fairlie, D. P. A refined agonist pharmacophore for protease activated receptor 2. *Bioorg. Med. Chem. Lett.* **2007**, *17*, 5552–5557.
- (65) Gardell, L. R.; Ma, J. N.; Seitzberg, J. G.; Kanpp, A. E.; Schiffer, H. H.; Tabatabaei, A.; Davis, C. N.; Owens, M.; Clemons, B.; Wong, K. K.; Lund, B.; Nash, N. R.; Gao, Y.; Lamah, J.; Schmelzer, K.; Olsson, R.; Burstein, E. S. Identification and Characterization of Novel Small-Molecule Proteinase-Activated Receptor 2 Agonists. *J. Pharmacol. Exp. Ther.* **2008**, *327*, 799–808.
- (66) Seitzberg, J. G.; Knapp, A. E.; Lund, B. W.; Mandrup Bertozzi, S.; Currier, E. A.; Ma, J. N.; Sherbukhin, V.; Burstein, E. S.; Olsson, R. Discovery of Potent and Selective Small-Molecule PAR-2 Agonists. *J. Med. Chem.* **2008**, *51*, 5490–5493.
- (67) Kawabata, A.; Saifeddine, M.; Al-Ani, B.; Leblond, L.; Hollenberg, M. D. Evaluation of Proteinase-Activated Receptor-1 (PAR1) Agonists and Antagonists Using a Cultured Cell Receptor Desensitization Assay: Activation of PAR2 by PAR1-Targeted Ligands. *J. Pharmacol. Exp. Ther.* **1999**, *288*, 358–370.